

TEXAS TRANSPORTATION INSTITUTE
TEXAS A&M RESEARCH FOUNDATION

TECHNICAL MEMORANDUM 605-4

TESTING PROGRAM

SAFETY PROVISIONS FOR SUPPORT STRUCTURES

ON OVERHEAD SIGN BRIDGES

By

D. L. Ivey, R. M. Olson, Eugene Buth, and T. J. Hirsch

Prepared for the Department of Transportation, Federal Highway Administration, Bureau of Public Roads, under Contract No. FH-11-7032. Financed with 1-1/2 percent HPR funds made available by the several States and administered by the Bureau of Public Roads.

Sponsored By

The States of Alabama, Arkansas, Connecticut, Florida, Georgia, Hawaii, Kentucky, Louisiana, Maryland, Michigan, Mississippi, Montana, Nebraska, New Hampshire, New Mexico, Rhode Island, South Dakota, Tennessee, Texas, West Virginia, Wyoming, and the District of Columbia.

The opinions, findings and conclusions expressed in this publication are those of the authors and not necessarily those of the Bureau of Public Roads and/or those of the State Highway Departments.

NOTE: For the reader who is interested in gaining a general idea of the value of the safety features of the overhead sign bridge and not in the details necessary to document the technical aspects of the study, the writers recommend reading page 1 and scanning the photographs in this report.

December 1969

TABLE OF CONTENTS

	Page
LIST OF FIGURES	iii
LIST OF TABLES	vi
* * * * *	
INTRODUCTION	1
DETAILS OF INDIVIDUAL TESTS	7
VEHICLE CRASH TESTS	7
Preliminary Test 605-Y	7
Regular Crash Test Series	13
<i>Test 605-A</i>	13
<i>Test 605-B</i>	16
<i>Test 605-C</i>	24
STATIC LOAD TESTS	30
Test 605-S1	30
Test 605-S2	34
LOWER CONNECTION LABORATORY TESTS	42
Tests 605-LC	42
* * * * *	
APPENDICES	
A TEST DATA	A1
B DETERMINATION OF TORSIONAL STIFFNESS COEFFICIENTS .	B1
Equilibrium Equations	B2
Compatibility Equations	B3

LIST OF FIGURES

Figure		Page
1	Prototype Overhead Sign Bridge -- Supports are designated A, B, C and D	2
2	Vehicle Before Test 605-Y	8
3	Vehicle After Test 605-Y	8
4	Support Base Before Test 605-Y	9
5	Support Base After Test 605-Y	9
6	Sequential Photographs of Test 605-Y	10
7	Sequential Photographs of Test 605-A	12
8	Vehicle Before Test 605-A	14
9	Vehicle After Test 605-A	14
10	Energy Absorbers	17
11	Energy Absorber Bolted in place on Lower Truss Chord at Support A	17
12	Energy Absorbers at Support B Before Test 605-B	18
13	Energy Absorbers at Support B After Test 605-B	18
14	Sequential Photographs of Test 605-B	20
15	Vehicle Before Test 605-B	22
16	Vehicle After Test 605-B	22
17	Impact Area After Test 605-B	23
18	Vehicle Damage, Test 605-B	23
19	Vehicle Before Test 605-C	25
20	Vehicle After Test 605-C	25
21	Sequential Photographs of Test 605-C	27
22	Impact Area After Test 605-C	28

LIST OF FIGURES (Continued)

Figure		Page
23	Layout of Static Load Test (605-S1) Not to Scale . . .	31
24	Load-Slip Curve, Test 605-S1	32
25	Layout of Test 605-S2	35
26	Applied Moment Versus Truss Rotation	37
27	Torque-Rotation Relationship	38
28	Dead Load Test of Prototype Structure	40
29	Test Apparatus	44
30	Test 605 LC-9 in Progress	44
31	Detail of Keeper Plates	45
32	Load-Slip Curves, Tests 605 LC-1 through 3	47
33	Load-Slip Curves, Tests 605 LC-4 through 7	48
34	Load-Slip Curves, Tests 605 LC-8 through 10	50
35	Effect of Bolt Torque on Slip-Free Energy	52
36	Effect of Axial Load on Slip-Free Energy	52
37	Effect of Keeper Type on Slip-Free Energy	52
38	Comparison of Load-Slip Curves for Tests 605-S1 and 605 LC Series	55
39	Torn Keeper Plate Used in Test 605 LC-9	56

APPENDICES

A1	Longitudinal Accelerometer Data - Test 605-Y	A6
A2	Longitudinal Accelerometer Data - Test 605-A	A8
A3	Longitudinal Accelerometer Data - Test 605-B	A9
A4	Longitudinal Accelerometer Data - Test 605-C	A10

LIST OF FIGURES (Continued)

Figure		Page
B1	Torsional Loads on OSB Truss	B2
B2	Torsional Displacements of OSB Truss	B3
B3	Model Used to Calculate K_s	B5
B4	Torque-Rotation Relationship	B9

LIST OF TABLES

Table		Page
1	SUMMARY OF TESTS CONDUCTED AS OF JANUARY 1, 1970	3
2	VEHICLE CRASH TEST CONDITIONS	4
3	SUMMARY OF VEHICLE CRASH TEST RESULTS	5
4	VEHICLE CRASH TEST INSTRUMENTATION	6
5	INSTRUMENTATION FOR STATIC LOAD TESTS OF OSB	41
6	LOWER CONNECTION LABORATORY TESTS	43

APPENDICES

A1	TEST 605-Y -- High Speed Film Data	A2
A2	TEST 605-A -- High Speed Film Data	A3
A3	TEST 605-B -- High Speed Film Data	A4
A4	TEST 605-C -- High Speed Film Data	A5

INTRODUCTION

Following the erection of the Overhead Sign Bridge, which was completed on September 8, 1969, an experimental program was begun which included both static load testing and dynamic vehicle crash tests. The purpose of the testing program was the experimental evaluation of the various factors which influence the forces acting on impacting vehicles and the reaction of the Overhead Sign Bridge to the loads imposed during collision events. Figure 1 shows the completed structure and gives a letter designation (A through D) to each support.

Table 1 outlines the tests which have been conducted to date. There have been two static load tests and four vehicle crash tests on the prototype structure. In addition, a series of ten tests has been conducted on a full-scale model of the lower support connection. The various factors which influenced the connection's resistance to an applied shearing load were determined by these tests. The purpose of each individual test is given in Table 1 and details of each test are given on pages 7 et seq. The analysis of these tests indicates that the following tentative conclusions may be drawn:

1. Static load tests and dynamic crash tests show that the break-away safety features of the truss will operate adequately to greatly reduce the forces on impacting vehicles.
2. Extrapolation of data from Static Test 605-S2 and the torsion analysis indicates that the Overhead Sign Bridge as modified with steel tube impact attenuators, can successfully sustain a 60-mph head-on hit by a 5000-pound vehicle without severe structural damage. (The most severe vehicle crash test which has been conducted was a 4090-lb Ford traveling 46.5 mph.)

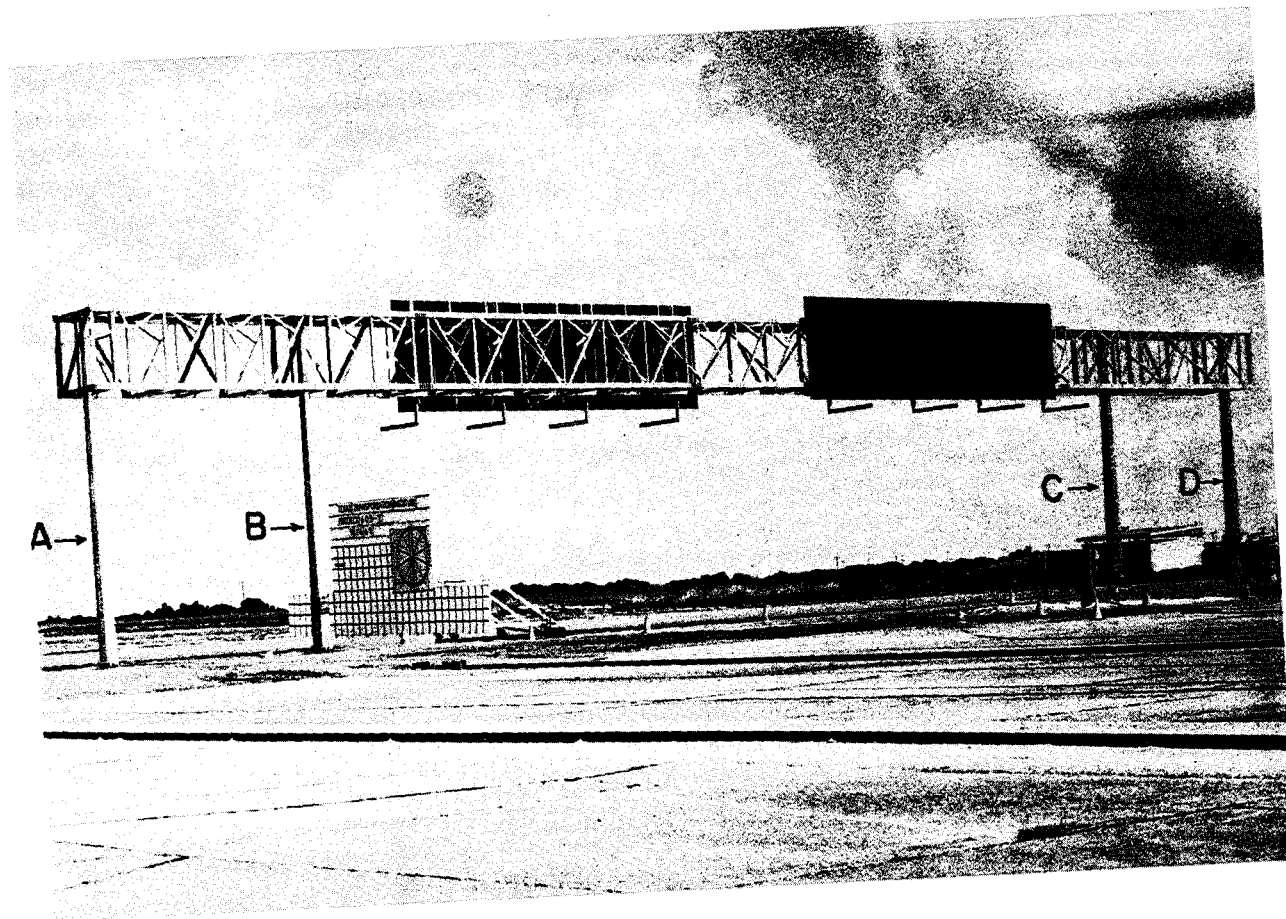


Figure 1, Prototype Overhead Sign Bridge
Supports are designated A, B, C and D.

TABLE 1

SUMMARY OF TESTS CONDUCTED AS OF JANUARY 1, 1970

<u>Test No.</u>	<u>Type</u>	<u>Date</u>	<u>Support</u>	<u>Orientation of Static Load or Impacting Vehicle</u>	<u>Purpose</u>
605-S1	Static Load	Sept. 11 1969	D	Head-On	Check on static resistance of break-away connections.
605-S2	Static Load	Nov. 12	A	Head-On	Determination of torsional stiffness characteristics of Overhead Sign Bridge (OSB).
605-Y	Vehicle Crash	Sept. 16	A	Head-On	Check of break-away concept under vehicle impact.
605-A	Vehicle Crash	Sept. 22	A	Head-On	First of a series of vehicle impact tests to evaluate per- formance of OSB.
605-B	Vehicle Crash	Dec. 11	B	Head-On	Check on the ability of mechan- ical energy dissipators and truss components to absorb excess support energy.
605-C	Vehicle Crash	Dec. 16	B	Head-On	Check on the ability of mechan- ical energy dissipators and truss components to absorb excess support energy.
605 LC Series 1 - 10	Lower Connection Static Load	Nov. 26 through Dec. 20	Laboratory Model	Head-On	Determination of the influence of bolt torque, axial load and keeper condition on the shear resistance of the lower support connection.

TABLE 2

VEHICLE CRASH TEST CONDITIONS

TEST NO.	VEHICLE	SPEED	TARGET	BREAK-AWAY CONDITION
605-Y	1963 Plymouth 3520 lbs	20.9 mph	Head-On Support A	No bolt keeper plate, Lower bolt torque: 100 ft-lbs, Upper bolt torque: finger tight.
605-A	1963 Ford 3950 lbs	25.7 mph	Head-On Support A	28 gage keeper plate, Lower bolt torque: 200 ft-lbs, Upper bolt torque: 10 ft-lbs.
605-B	1959 Simca 2100 lbs	44.0 mph	Head-On Support B	28 gage keeper plate, Lower bolt torque: 200 ft-lbs, Upper bolt torque: 10 ft-lbs.
605-C	1963 Ford 4090 lbs	46.5 mph	Head-On Support B	28 gage keeper plate, Lower bolt torque: 200 ft-lbs, Upper bolt torque: 10 ft-lbs.

TABLE 3

SUMMARY OF VEHICLE CRASH TEST RESULTS

Test No. →	605-Y	605-A	605-B	605-C
Vehicle Weight, lbs	3520	3950	2100	4090
Initial Velocity, mph [*]	20.9	25.7	44.0	46.5
Change in Velocity, mph [*]	7.3	5.4	14.8 ^{**}	8.9
Average Deceleration, g's	2.8	3.1	9.6	6.7
Maximum Deceleration, g's	5.0	7.4	22.4	19.1
TARGET SUPPORT	A	A	B	B
Rotation [*]	55°	86°	65° ^{***}	63° ^{***}
Height of lower end of support at peak of swing, ft	9.4	18.5	13.5	10.5
SUPPORT	B	B	C	D
Maximum Stresses				
Bending in Flange, psi	4900	4200	12,800	6,700
Shear in Web, psi	2400	1400	150	760
Change in Axial Stress, psi	240	510	-	-
APPROXIMATE ROTATION OF TRUSS [*]	3°	2°	3°	1°

* From film data.

** Change in velocity over the period necessary to activate the break-away component of the support. Vehicle snagged on lower end of support post and was stopped.

*** Impact energy absorbers were installed following Test 605-A.

TABLE 4

VEHICLE CRASH TEST INSTRUMENTATION

Device	Location	Purpose
CAMERAS:		
1 Hycam (500 frames per sec)	West of sign leg	To record vehicle time-displacement.
1 Hycam (500 frames per sec)	West of sign leg	To record leg movement.
1 Fastax (500 frames per sec)	West of sign leg	To record truss movement.
1 Bell & Howell (128 fps)	West of sign leg	For overall documentary.
*1 Fairchild Gun Camera (24 fps)	In vehicle	To record "passenger" view out windshield.
ACCELEROMETERS:		
1 Statham	Right longitudinal vehicle frame member***	To sense longitudinal acceleration.
1 Statham	Left longitudinal vehicle frame member***	To sense longitudinal acceleration.
1 Impact-O-Graph	Floor of vehicle baggage compartment	To sense and record triaxial accelerations.
STRAIN GAGES: **		
1 Semiconductor Gage	South flange of adjacent leg	To sense bending in adjacent leg.
1 Semiconductor Gage	North flange of adjacent leg	To sense bending in adjacent leg.
2 Semiconductor Gages	Web of adjacent leg	To sense shear in adjacent leg.
OTHER:		
1 Pair of Tape Switches	In front of struck leg	To sense initial velocity.
1 Pair of Tape Switches	Behind struck leg	To sense final velocity.
1 Tape Switch	On flange of struck leg	To sense impact.
1 Tape Switch and flash bulb	On vehicle	To indicate impact visually.
*1 Seat Belt Strain Gage	Attached to seat belt	To sense seat belt force on Alderson Articulated Anthropometric Dummy.

*Used on Test 605-A only.

**Not recorded on tests of Support B.

***Positioned directly behind front seat.

DETAILS OF INDIVIDUAL TESTS

VEHICLE CRASH TESTS

One preliminary and three regular full-scale vehicle crash tests were conducted between September 16 and December 16, 1969. A summary of the test conditions and test results is given in Tables 2 and 3. Individual tests are discussed in the following paragraphs.

Preliminary Test 605-Y

As a preliminary check of the "break-away" capabilities of the Overhead Sign Bridge (OSB) before beginning the evaluation and development (regular) series, a 1963 Plymouth traveling 20 mph was directed head-on into Support A, the outside left support. The details of test conditions and results are given in Tables 2 and 3. This test was conducted primarily to confirm estimated fracture strength of the upper bolted connection, and secondarily to observe the overall system. Lower bolt torque was 100 ft-lbs and no bolt keeper plate was installed at the break-away base. Upper bolts, at the connection to the upper chord, were finger-tight.

The system functioned as designed, and the results checked with the mathematical simulation* very closely. The support rotated up and away from the vehicle through an angular displacement of 55°. The vehicle passed underneath after sustaining only minor damage. Figures 2 through 5 show selected photographs of the vehicle and OSB before and after the test. Based on this test, the functioning of the "break-away" components was verified and the reliability of the simulation was indicated.

* "Mathematical Simulation and Correlation," J.E. Martinez, J.J. Jumper, and F.Y. Baskurt, Technical Memorandum 605-2. Texas Transportation Institute, January 1970.



Figure 2, Vehicle Before Test 605-Y.



Figure 3, Vehicle After Test 605-Y.

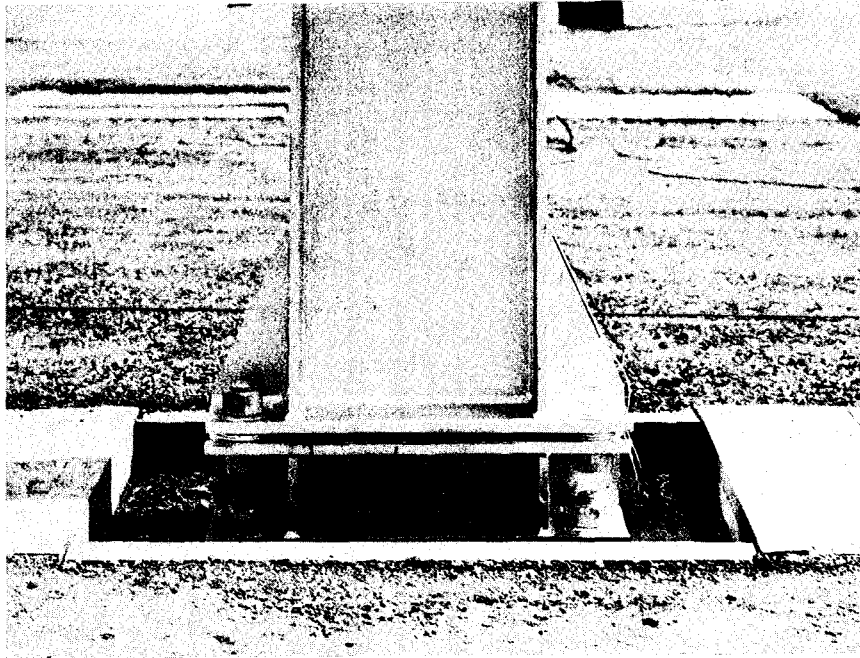


Figure 4, Support Base Before Test 605-Y.

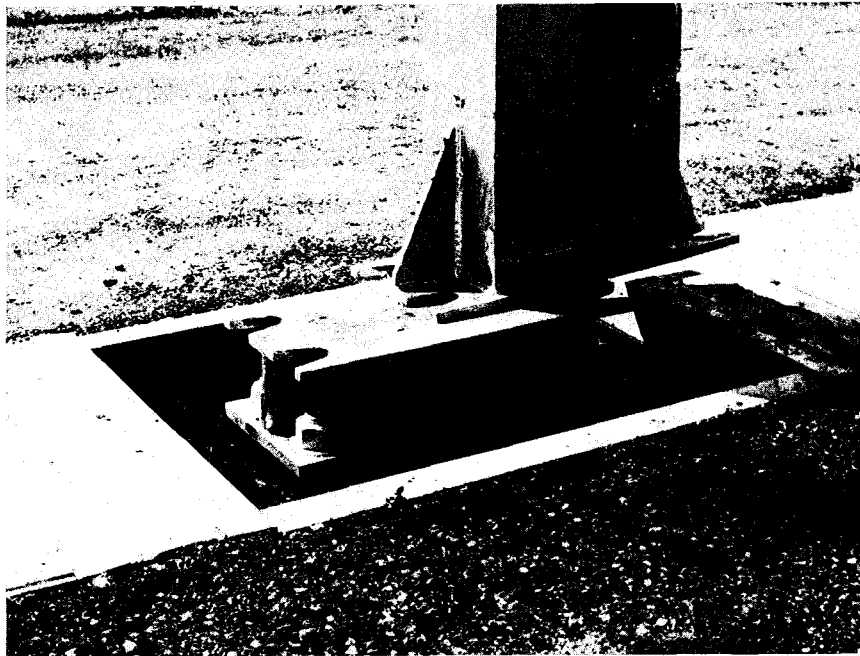
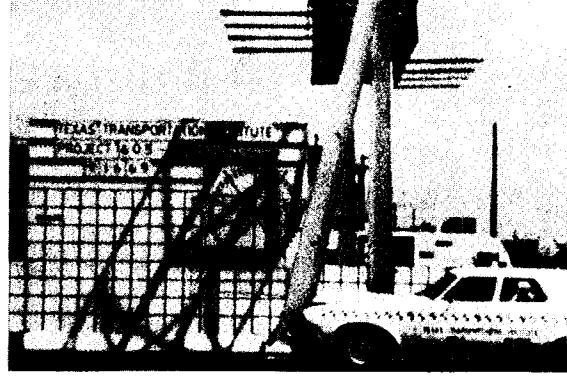


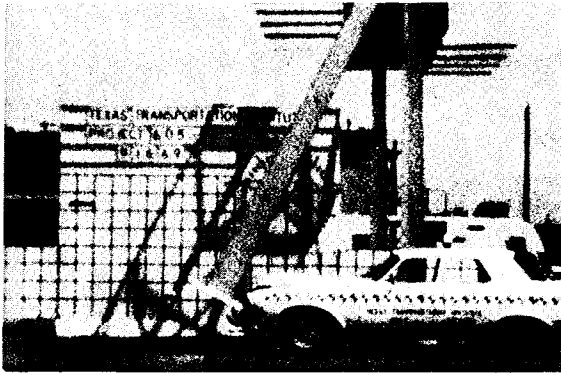
Figure 5, Support Base After Test 605-Y.



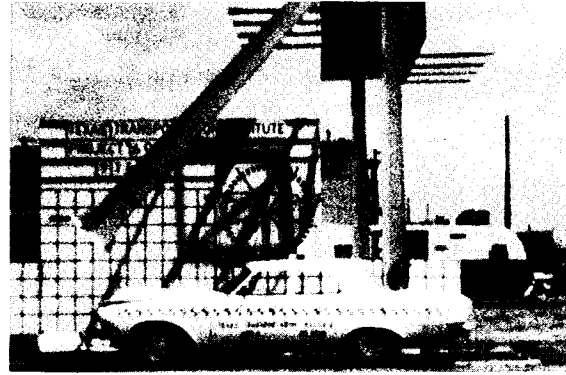
t = 0 sec



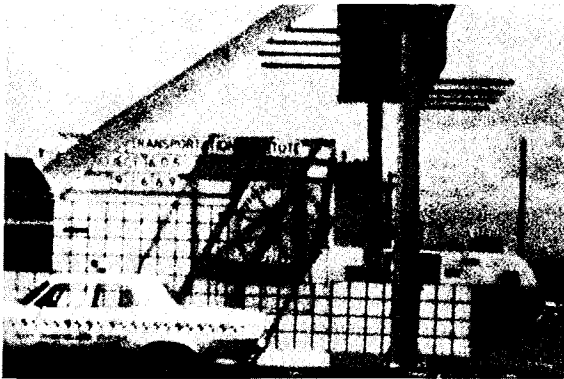
t = .223 sec



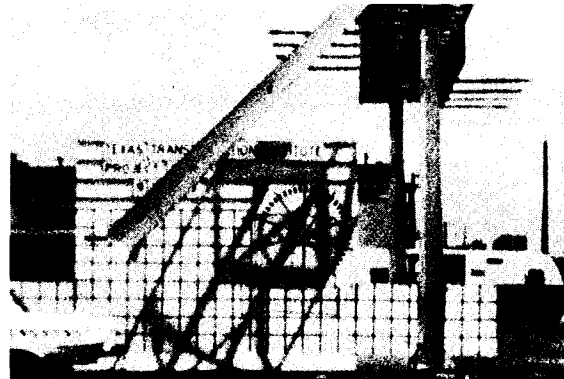
t = .426 sec



t = .730 sec



t = 1.237 sec



t = 1.673 sec

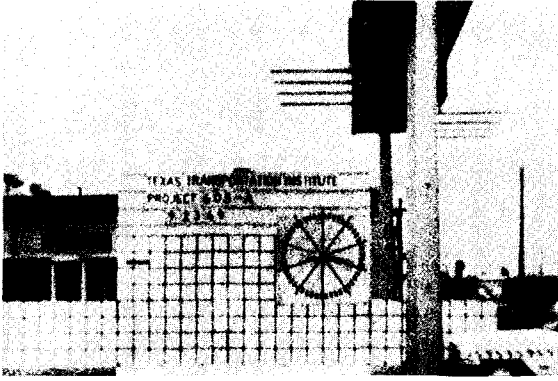
Figure 6, Sequential Photographs of Test 605-Y.

Frame by frame analysis of the data films revealed that the break-away base became disengaged at 0.040 seconds after impact; and that the support post and vehicle were in contact for 0.125 seconds. The average speed reduction during time of contact was 7.3 miles per hour. The sequence photographs shown in Figure 6 clearly illustrate that the support post clears the colliding vehicle adequately.

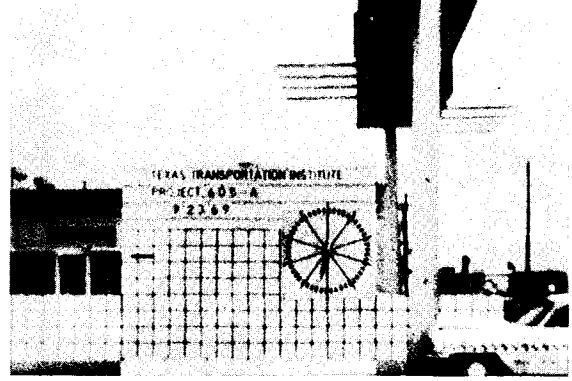
The test conditions in this preliminary test were less severe than in the regular test series (see Table 2). A comparison of vehicle-support behavior as predicted by mathematical simulation with crash test data follows:

	<u>Rigid Dynamic Model*</u>	<u>Crash Test 605-Y</u>
Time in Contact (sec)	0.113	0.125
Velocity Change (mph)	6.8	7.3
Average g's	2.7	2.8
Maximum Rotation (deg)	64.0	55.0

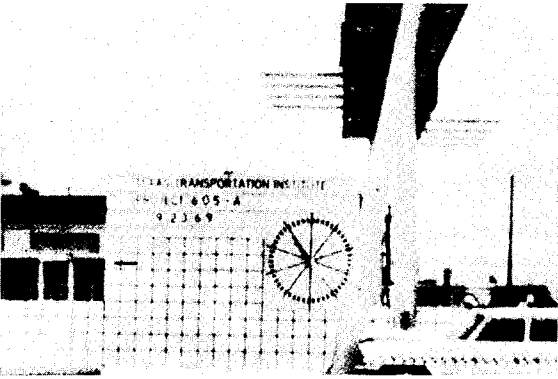
* See Technical Memorandum 605-2.



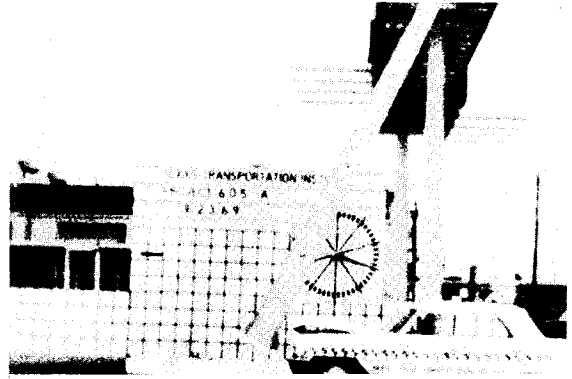
t = 0 sec



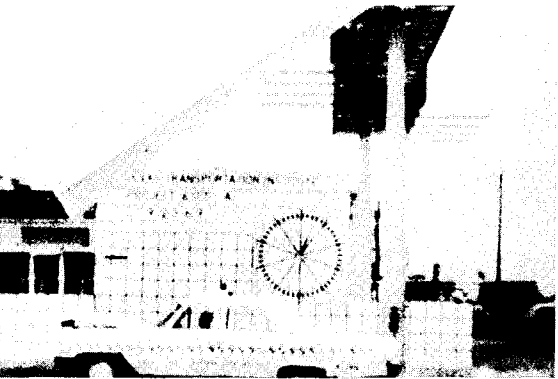
t = .044 sec



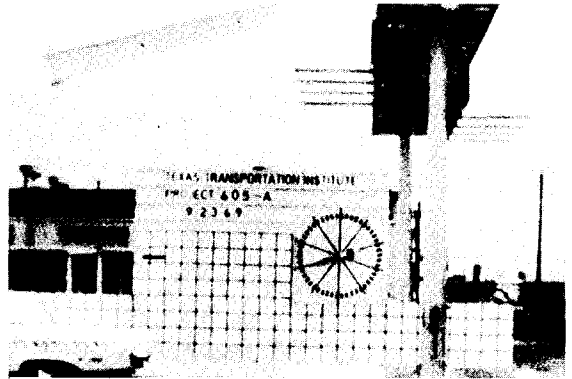
t = .127 sec



t = .283 sec



t = .627 sec



t = 1.144 sec

Figure 7, Sequential Photographs of Test 605-A.

Regular Crash Test Series

Test 605-A

The first vehicle crash test in the regular evaluation and development program was conducted on September 23, 1969 on the first day of Project Policy Committee Meeting Number 2. A 1963 Ford impacted the outside left support at a velocity of 25.7 mph. Tables 2 and 3 summarize the test conditions and results. Support resistance was expected to be greater than in Test 605-Y since the lower bolt torque was increased to 200 ft-lbs and a 28-gage keeper plate was installed. Preliminary calculations and observations of test films led to the conclusion that the bolt keeper plate and increased base bolt torque used in Test 605-A did not appreciably affect the vehicle-support behavior. These conditions (28-gage bolt keeper plate, and 200 ft-lbs base bolt torque) were established for the remainder of the regular crash test series.

The reaction of the support was again as predicted by the mathematical simulation. The support rotated through 83° (observed), allowing the vehicle to pass underneath. Damage to the vehicle was similar to that of Test 605-Y. Figure 7 shows sequential photographs of the interaction of vehicle and OSB during the test. Figures 8 and 9 show the vehicle before and after the test. A comparison of test results of 605-Y and 605-A, presented in Table 3, indicates that average deceleration increased 11 percent and maximum deceleration increased about 47 percent. The change in velocity was less than in the preliminary 20 mph test (605-Y).



Figure 8, Vehicle Before Test 605-A.



Figure 9, Vehicle After Test 605-A.

A comparison of vehicle-support behavior as predicted by mathematical simulation with crash test data follows:

	Computer Simulation Rigid Dynamic Model*		Crash Test 605-A	
Vehicle Weight (lbs)	3960			
Initial Vehicle Velocity (mph)	25.7	F		
Base Resistance (kips)	7.0	D		
Resistance at Shear Connection (kips)	17.0	R		

Time in Contact (sec)	0.091	N	0.079	D
Velocity Change (mph)	5.9	D	5.4	E
Average g's	2.95	R	3.1	V
Maximum Rotation (deg)	81.5	F	83.0	R
Comment	Post hit truss with $E_k = 3.1'k$	D	Post hit truss.	E
		O		S
		O		B
				O

* See Technical Memorandum 605-2.

Test 605-B

In evaluating the break-away features of the Overhead Sign Bridge and the functioning of the bridge structure, two distinct areas of interaction are apparent. One, the interaction of the vehicle with the support; and two, the interaction of the rotating OSB support with the lower chord members of the truss. The first two tests showed that the interaction of the vehicle with the support leg could be predicted with reasonable accuracy by use of the computer simulation. A matter of major concern then became the interaction of the rotating support with the truss. For vehicle velocities greater than 25 mph, the computer simulation predicted that the support would possess a significant amount of kinetic energy when it impacted the lower chords of the truss. The protection of the lower chord members by distributing the impact force, as well as the dissipation of this excess energy, was carefully considered. To provide the required distribution and dissipation, a steel tube energy absorber was designed which could be placed to protect the lower chord members of the truss. Static laboratory and field tests were run to verify the function of these energy absorbers before crash tests were conducted. A closeup of this energy absorber before it was placed on the truss is shown in Figure 10. The energy absorbers installed on the truss are shown in Figures 11 and 12. Selection of the channel sections was made (1) to provide adequate load distribution to the truss, and (2) to provide a flat bearing surface for the cylindrical tubes during impact loading. The design of the connection provided both conditions, as can be seen in Figure 13. No damage to the lower chord occurred and the energy absorbers were crushed against the channel sections.

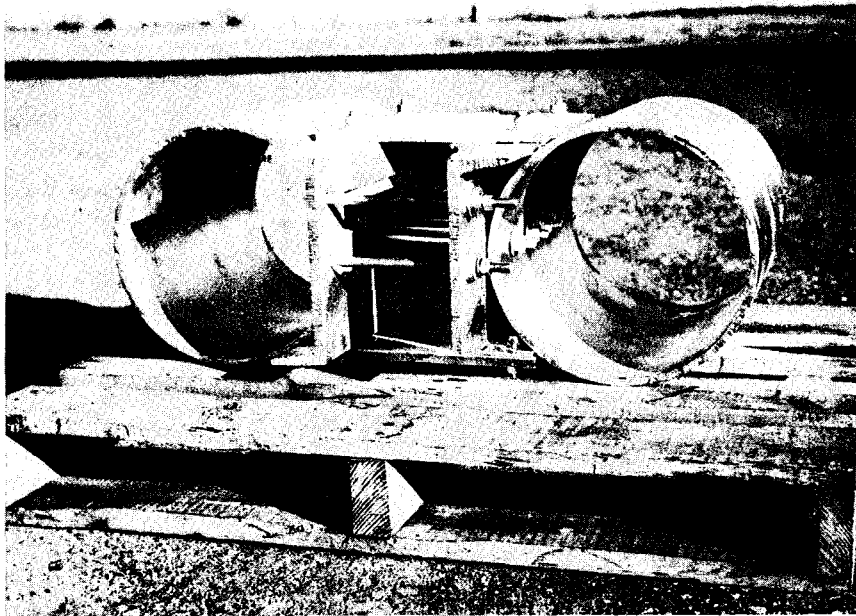


Figure 10, Energy Absorbers
(Steel tubing: $\frac{3}{8}$ in. wall thickness,
12 in. diameter, 17 inches long).

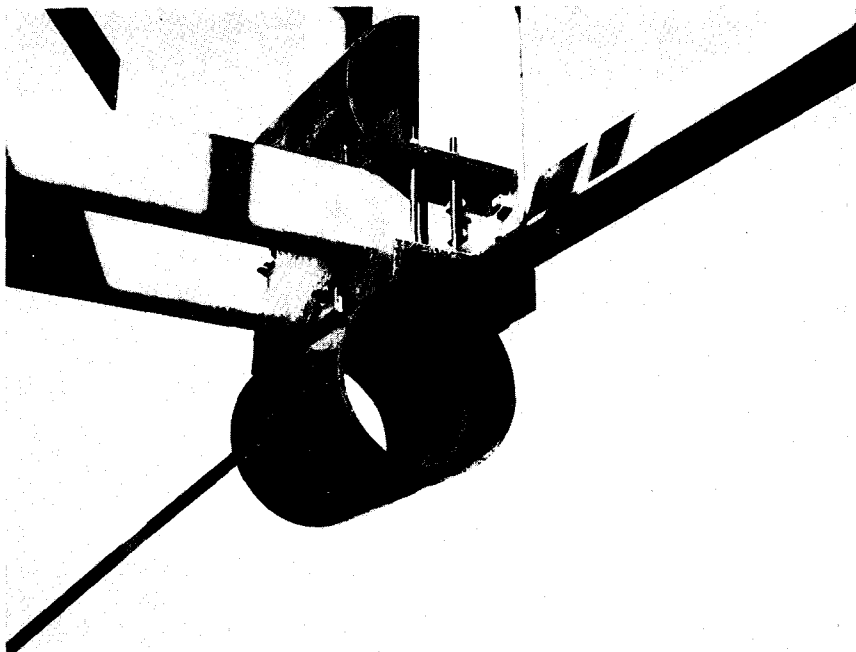


Figure 11, Energy Absorber
Bolted in place on
Lower Truss Chord at Support A.



Figure 12, Energy Absorbers at Support B Before Test 605-B.

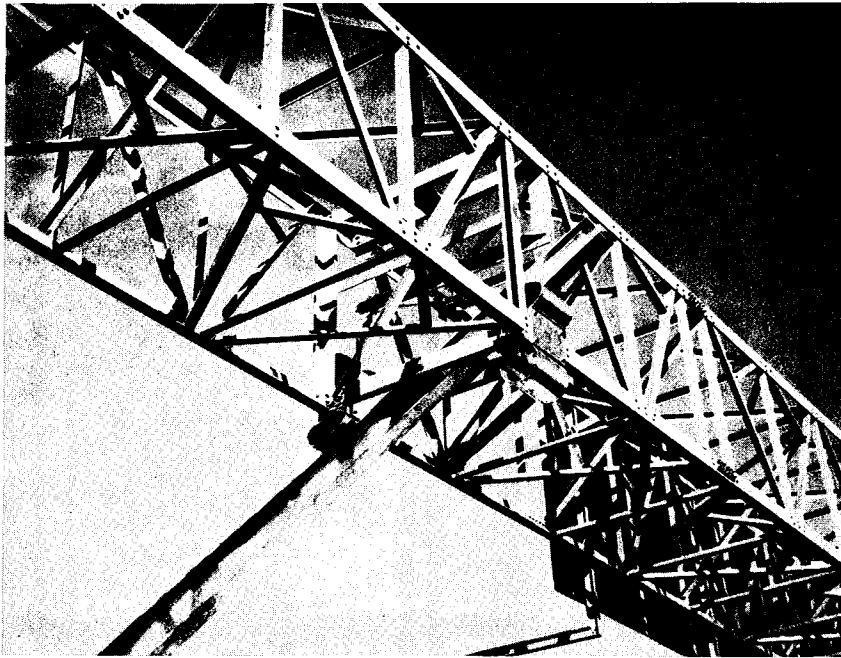
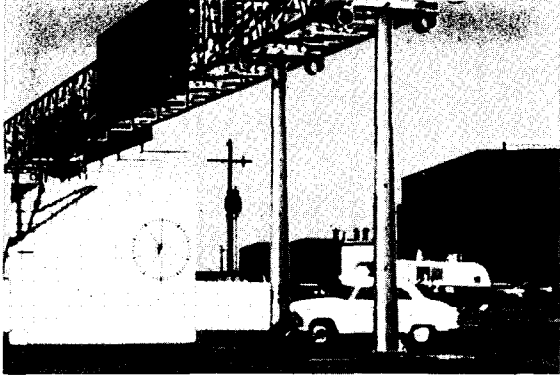
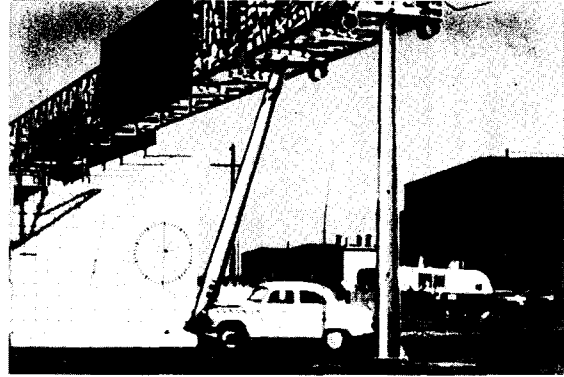


Figure 13, Energy Absorbers at Support B After Test 605-B.

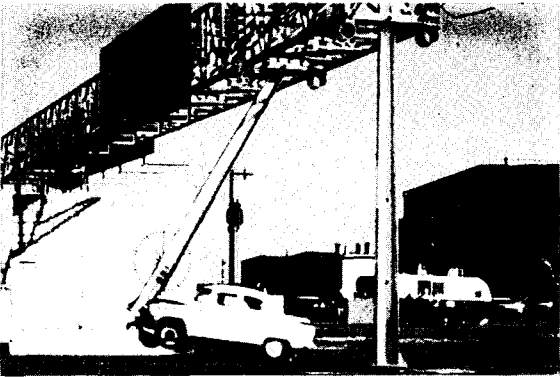
Using an analysis of the OSB subjected to torsional loads (Appendix B) and the empirical data developed in static load tests 605-S2, the torsional stiffness coefficients for various components of the Overhead Sign Bridge were determined. Using these coefficients, the amount of energy which the truss could be expected to absorb without shearing all top connection bolts was estimated to be 145 Kip-Ft. However, it was decided that the validity of this analysis should be tested and that the energy level of the impacting vehicle, and therefore the energy of the subsequently rotating support, should be increased gradually until the dynamic functioning of the tube energy absorbers and the energy absorption capability of the OSB was further verified. For this reason, the speed of the impacting vehicle in Test 605-B was increased to 44 mph. A 1959 Simca weighing 2100 lbs was used in this test to gain some appreciation of the interaction between the truss and a compact vehicle. The truss and support conditions were the same as in Test 605-A.



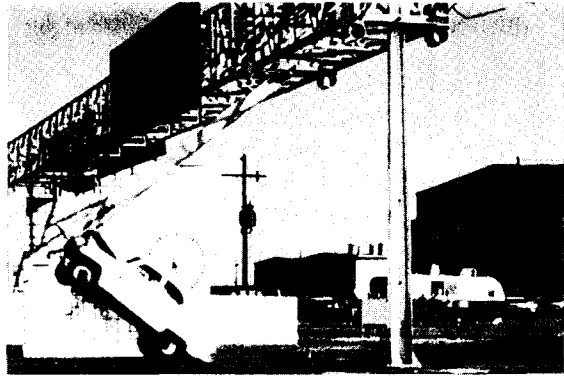
t = 0 sec



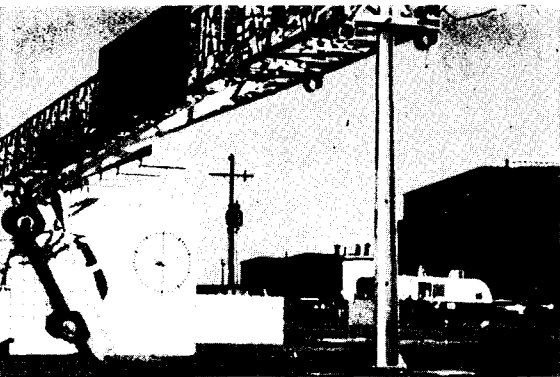
t = .117 sec



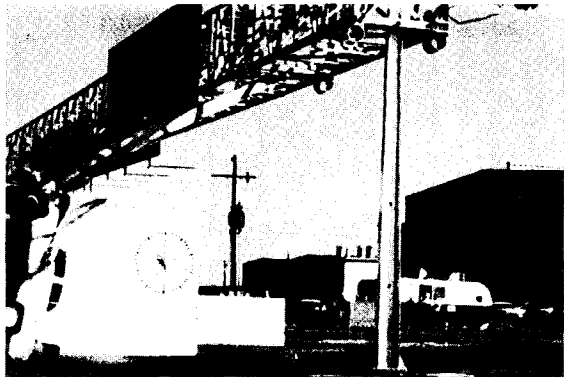
t = .195 sec



t = .351 sec



t = .468 sec



t = .781 sec

Figure 14, Sequential Photographs of Test 605-B.

A very unexpected condition occurred during Test 605-B: The vehicle remained in intimate contact with the support after initial contact. This interaction of vehicle and support is shown by the sequence photographs of Figure 14. The front of the vehicle was deformed significantly by the impact with the support, remained in contact with the support, and was lifted at the front end by the support, finally wedging itself between the ground and support in a vertical position. The major reason for this behavior is believed to be that the front of the Simca is relatively soft compared to the larger automobiles tested. This front end "deformability" allowed the post to penetrate 21 inches in toward the motor while bending the frame's front cross member. The bending of this cross member forced the two longitudinal members to come together, thus clamping the support in the pincer-type action of the vehicle's front structure. This pincer action prevented the support from springing away from the vehicle after the "break-away" connections at the bottom and top sheared. As the support rotated, while maintaining contact with the Simca, the elevation of the support base plate increased. The slotted projections of this base plate (see Figure 5) acted as a fork which caught the front end of the Simca and raised it to the maximum elevation shown at $t = 0.781$ seconds in Figure 14.

Even though the interaction of vehicle and post after the initial shearing of the lower support was rather unexpected, the damage to the vehicle was not more than had been expected and the decelerations that the vehicle experienced were not excessive. The average deceleration (from accelerometer traces) during the period necessary to activate the break-away component of the support was 9.6 g's over 0.068 seconds, producing a change in velocity of 21.5 feet per second or 14.6 miles per hour. The maximum deceleration was rather high, 22.4 g's.



Figure 15, Vehicle Before Test 605-B.



Figure 16, Vehicle After Test 605-B.

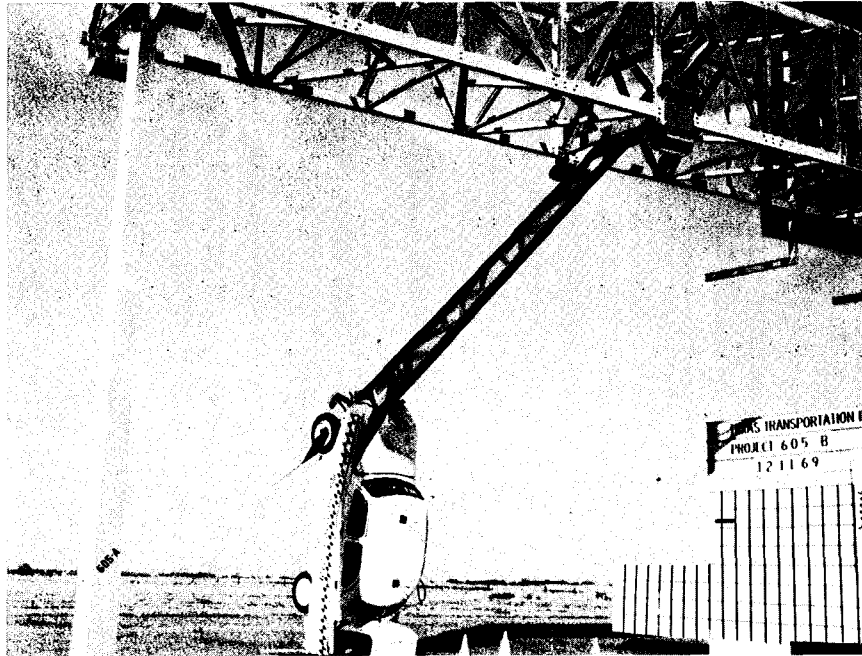


Figure 17, Impact Area After Test 605-B.

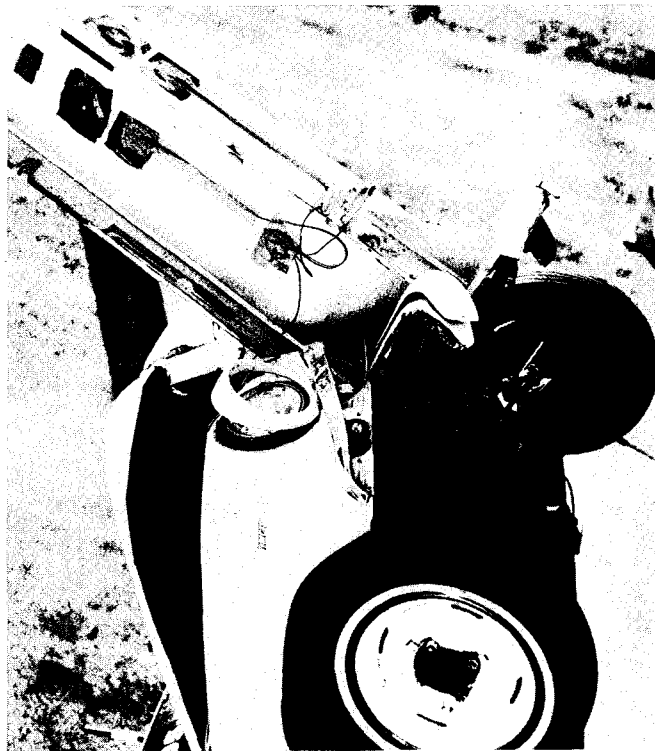


Figure 18, Vehicle Damage, Test 605-B.

The deceleration traces are shown in Appendix A, as well as a tabulation of photographic data. Due to the complex nature of the vehicle-post interaction, good estimates of the energy dissipated by the energy absorbers and Overhead Sign Bridge are not obtainable. The energy absorbers did function as expected, there was no significant damage to the truss, and the stresses in Supports C and D were nominal.

Comparison of mathematical simulation prediction and crash test information has not been accomplished at this time.

Test 605-C

In an effort to provide a more critical test of the energy absorption capabilities of the Overhead Sign Bridge and to determine the interaction of a medium-sized vehicle at moderate speed, Test 605-C was performed. The 4090 lb 1963 Ford impacted Support B head-on at a velocity of 47 mph. The interaction of vehicle with post was as expected and a nominal vehicle damage is shown by Figure 20. The average deceleration during contact with the support was 6.7 g's and the peak deceleration was 19.1 g's.

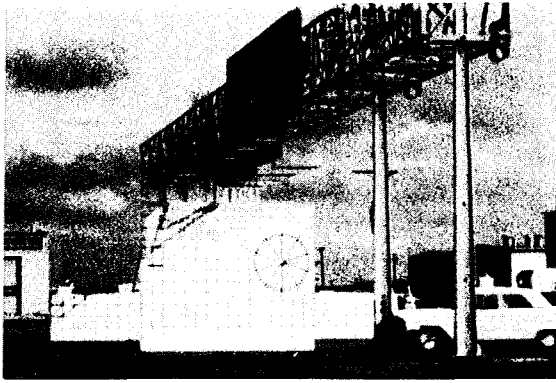


Figure 19, Vehicle Before Test 605-C.

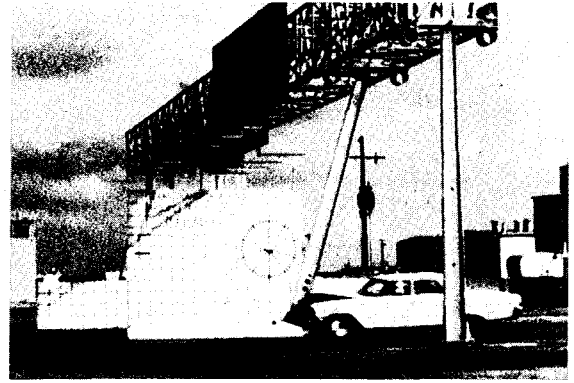


Figure 20, Vehicle After Test 605-C.

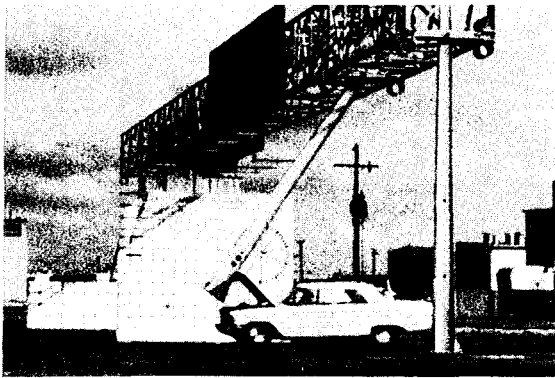
The break-away devices at the bottom and top of Support B functioned as predicted, allowing the support to rotate up and away from the vehicle. During the time from initial vehicle contact until the upper bolts sheared, the truss rotation was only approximately 1° . This was somewhat surprising since the previous 3 tests had shown truss rotations from 2° to 3° during this time. The vehicle passed under the support with a clearance of approximately 5.8 ft. After swinging through an angle of 50.5° , the support made contact with the energy absorbers and proceeded to crush them until the total support rotation had increased to 62.5° . During the crushing of the energy absorbers, the rotation of the truss was less than 1° .



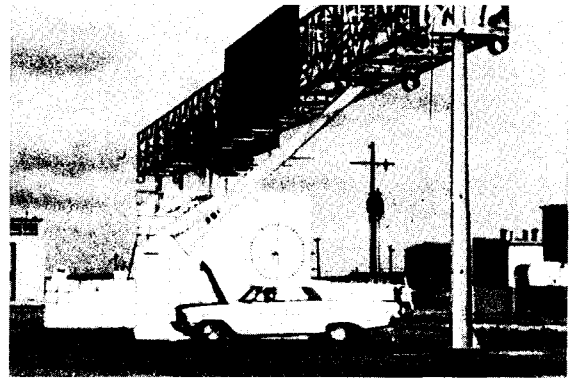
t = 0 sec



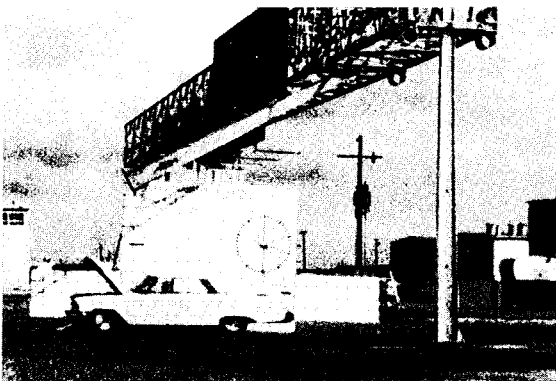
t = .078 sec



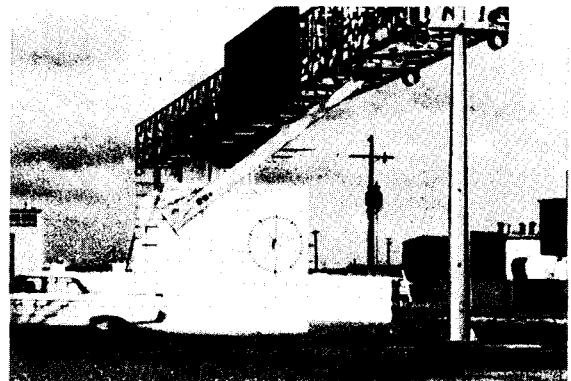
t = .156 sec



t = .234 sec



t = .336 sec



t = .492 sec

Figure 21, Sequential Photographs of Test 605-C.

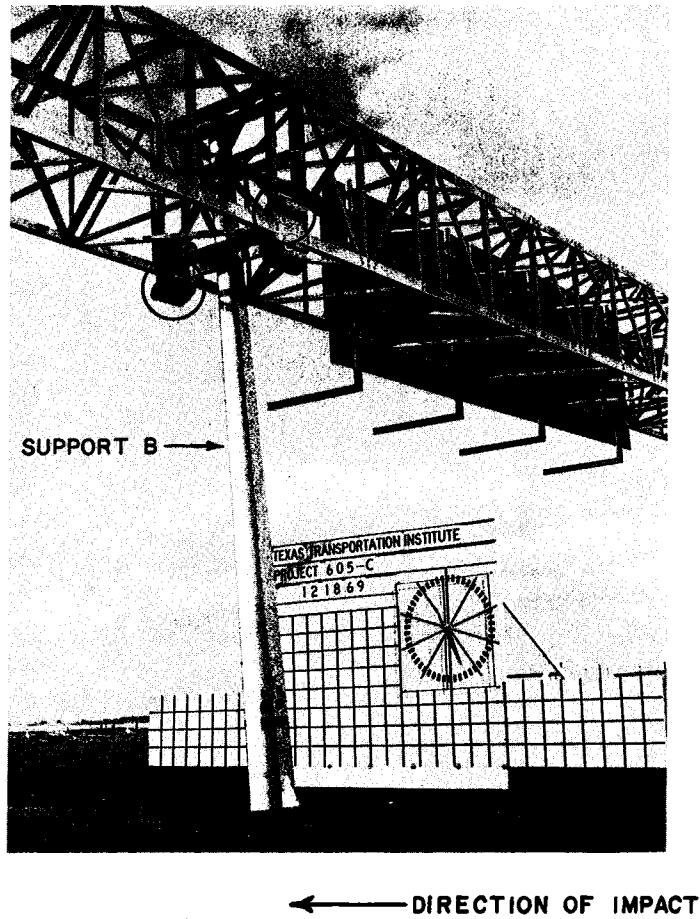


Figure 22, Impact Area After Test 605-C.
Note crushed energy absorbers,
(circled above),

Using photographic analysis, the angular velocity of the support was estimated to be 2.72 radians per second when contact was made with the energy absorbers. Using elementary equations of physics, the energy dissipated by the energy absorbers was calculated to be 23 Kip-Ft. Based on the static load analysis of Appendix B, it was estimated that the Overhead Sign Bridge could absorb 145 Kip-Ft of energy. Our estimates of support energy when contact is made between support and truss appear to be somewhat high. The 60-mph test of a 5000 lb vehicle which will take place in February 1970 should provide a critical test of the OSB's capacity for absorbing energy.

Comparison of mathematical simulation prediction and crash test information has not been accomplished at this time.

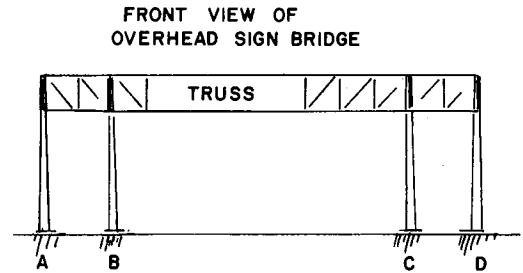
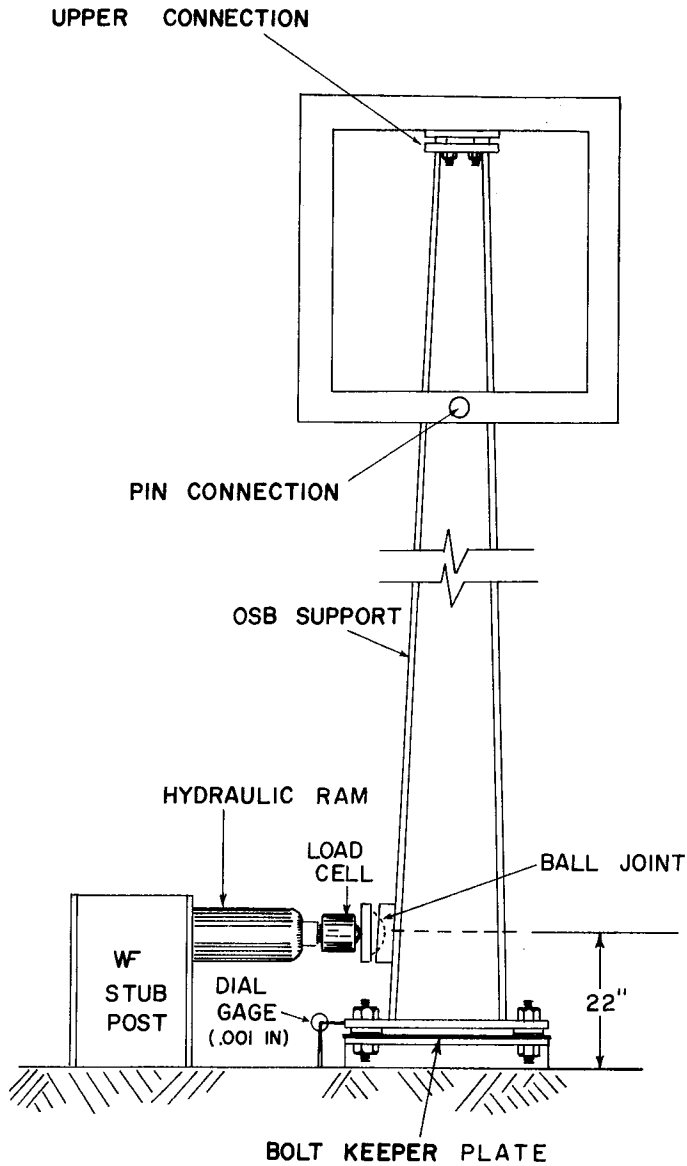
STATIC LOAD TESTS

Test 605-S1

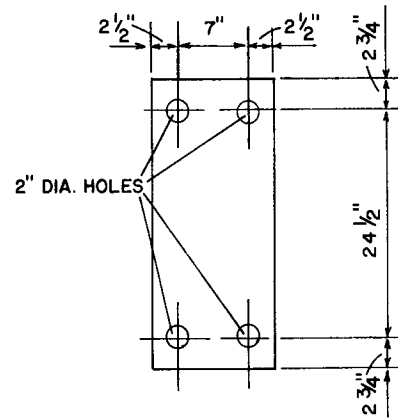
The first experiment performed on the Overhead Sign Bridge after erection was a static load test on Support D. The purpose of the test was to verify the functioning of the break-away connections at the top and bottom of one of the OSB supports.

To perform this test, a hydraulic ram was placed so that a load could be applied to Support D at the same point and in the same direction as the load applied by a vehicle impacting head-on. The test layout is shown in Figure 23. A gradually increasing load was applied to exterior Support D until the base slipped free; subsequently the four bolts at the upper connection were fractured.

The relationship observed between load and slip (base movement in the direction of the applied load) is shown in Figure 24. Initial slip of the base began at an applied load of slightly over 4,000 pounds. As the lower connection bolts came in contact with the 20 gage steel keeper plate, the load necessary to continue the slipping increased to a maximum of 17,000 pounds and then decreased abruptly as the bolts tore free of the keeper. After a slip of 4.5 inches, the support was completely free of the base plate. The load dropped to 2,000 pounds at this point and then increased gradually to 7,100 pounds when the upper connection bolts fractured. The dotted lines dividing the area under the curve in Figure 24 show a hypothesis concerning the energy attributed to each of the factors resisting base movement. The area designated as truss stiffness would include both truss flexural and torsional stiffness. The test indicated that both lower and upper



SUPPORT DESIGNATIONS



DETAIL OF BOLT KEEPER PLATE
(20 GA. STEEL)

FIGURE 23, LAYOUT OF STATIC LOAD TEST (605-SI).

NOT TO SCALE.

STATIC LOAD TEST - 605-SI
BOLT TORQUE - 50 FT. LBS.
KEEPER - 20 GA. STEEL

32

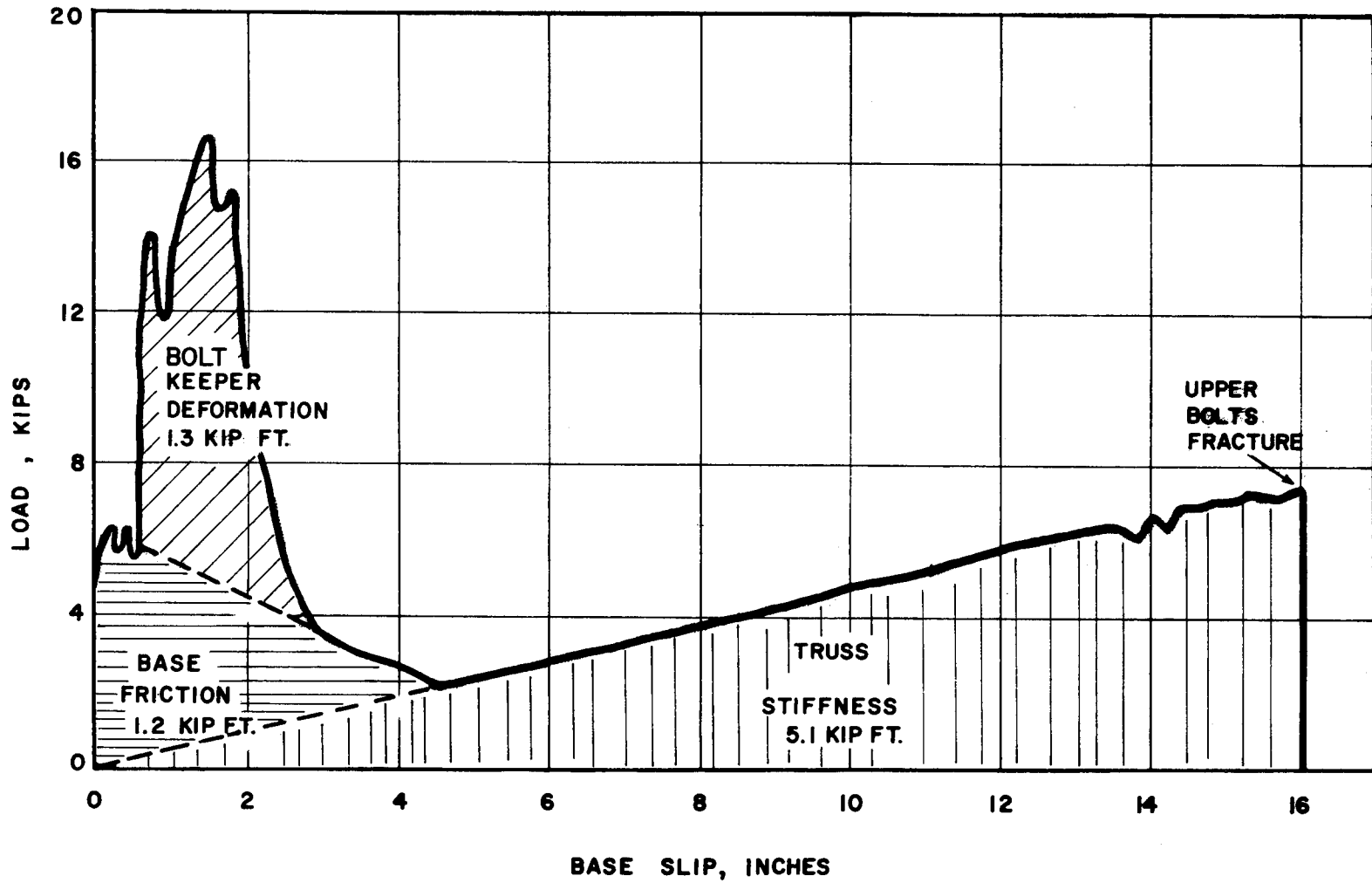


FIGURE 24, LOAD - SLIP CURVE, TEST 605-SI.

break-away connections functioned in an acceptable manner.

This static load test was conducted on a break-away support system consisting of:

1. bolted break-away base (bolt torque = 50 ft-lbs),
2. bolt keeper plate (thickness = 0.0299 in., 20 gage),
3. support column,
4. upper connection (4-1/2 in. diameter A307 bolts), and
5. OSB truss.

Each component of this system contributed to the load-slip characteristics shown in Figure 24. Estimates of the load required to overcome base friction, tear the keeper plate and fracture the upper connection bolts were made prior to conducting this test. The total force required to actuate the break-away system was higher than the estimates. As a result of this test, the load-slip characteristics of each component of the total system were more clearly defined.

Effect of bolt torque and keeper plate thickness were examined separately in a series of lab tests. These lab tests are described starting on page 43 of this Technical Memorandum.

Test 605-S2

One of the primary considerations that had to be reconciled before attempting a vehicle impact test at speeds in excess of 25 mph was the torsional stiffness characteristic of the various components of the Overhead Sign Bridge. An early theoretical analysis, based on some conservative assumptions, had indicated that the truss segment was extremely stiff and could take only very small torsional displacements before failure of all upper connection bolts would take place. It was considered necessary, in some way, to dissipate the excess energy of a leg which had been hit by a vehicle traveling at a relatively high velocity. If the leg was allowed to collide with the truss at the lower chord, it might damage the member. There are two means by which this energy may be dissipated: (1) by the placing of energy absorbers at the contact points between the rotating leg and the truss, and (2) by the torsional warping of the truss throughout its length. Another function that the energy absorber must perform is to satisfactorily distribute the impact load to the lower chord so that the chord is not fractured or otherwise excessively distressed. A limited amount of data developed on Test 605-S1 indicated that the truss might be significantly more flexible in the torsional displacement mode than the theoretical calculations had predicted. In order to determine if this was true, Test 605-S2 was set up to evaluate the torsional stiffness characteristic of the truss, to determine how the tubular energy absorbers would work, and to determine whether the channels would properly distribute the load applied on the tubular energy absorbers to the lower chords of the truss.

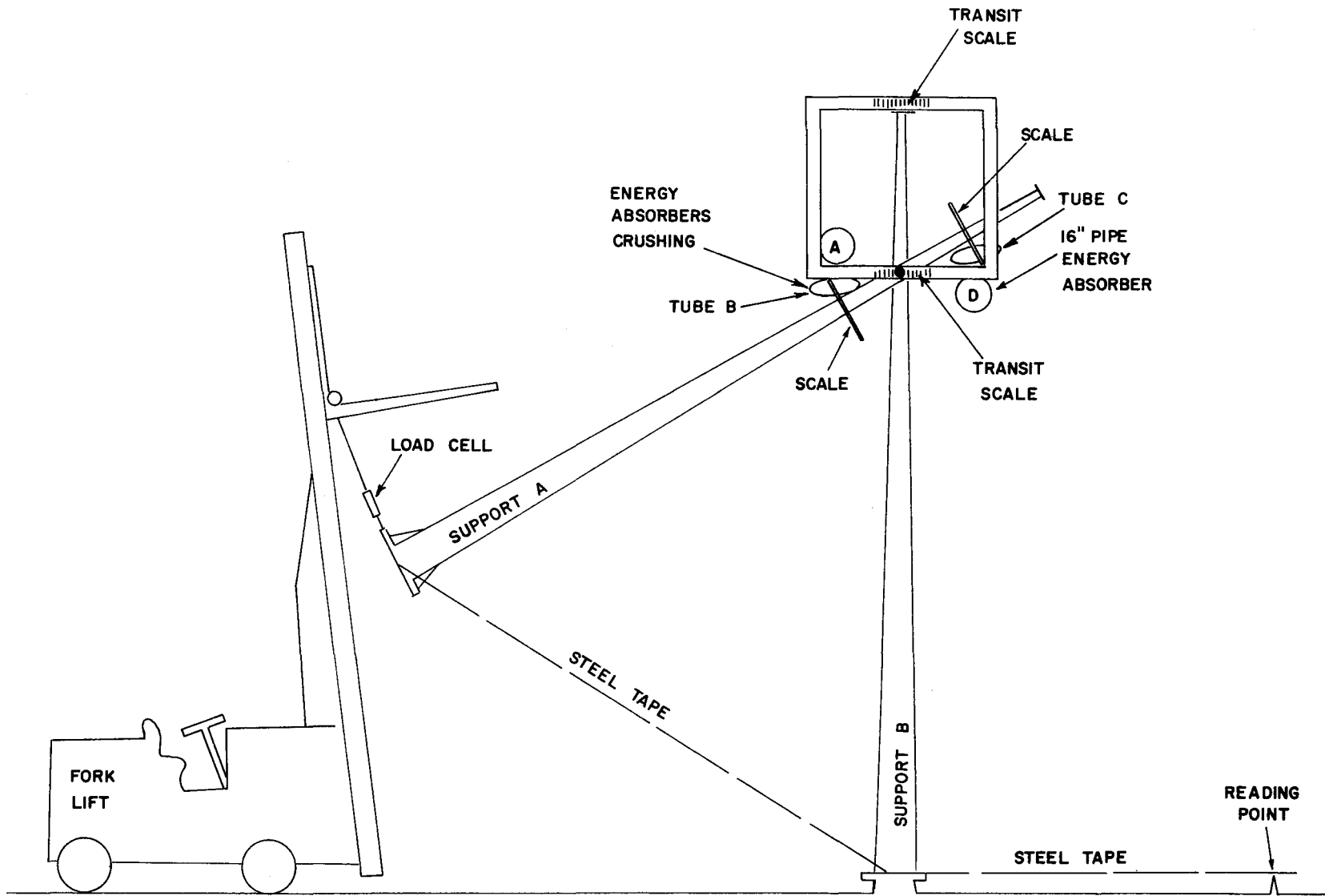
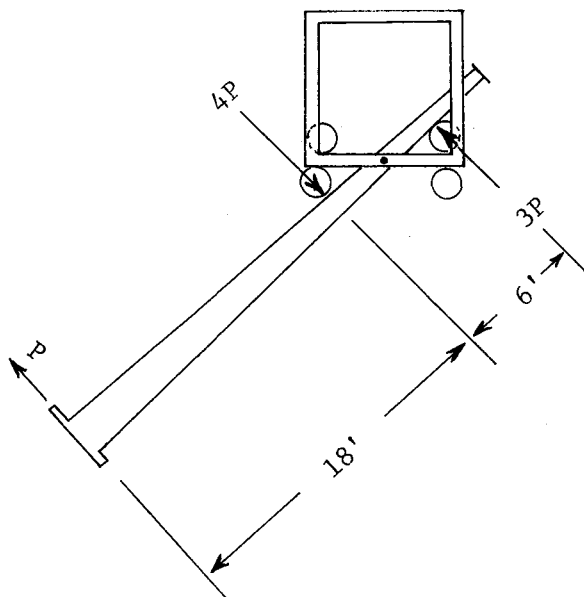


FIGURE 25, LAYOUT OF TEST 605-S2.

A layout of Test 605-S2 is given by Figure 25. Support A was detached at the base and rotated until contact was made with the tubes B and C. By attaching Support A to a fork lift, a load was applied which produced a rotation of Support A, crushing energy absorbers B and C and producing a torsional rotation of the truss elements. This load on Support A was increased progressively until the energy absorbers were completely crushed, and until the upper connection bolts at Support B failed. At this time, the load dropped off to 130 kip-ft and the rotation of Support A was again continued until the applied torque was equal to 190 kip-ft. The test was discontinued when the fork lift capacity (for vertical height) had been reached.

The applied load was assumed to bear on each cylindrical tube in the ratio shown below, and the resulting movement was calculated as:

$$M = 4P \times 3' + 3P \times 3' = P \times 21'$$



The computed moments versus truss rotation are plotted in Figure 26. A detailed analysis of the data in this test is given in Appendix B. The

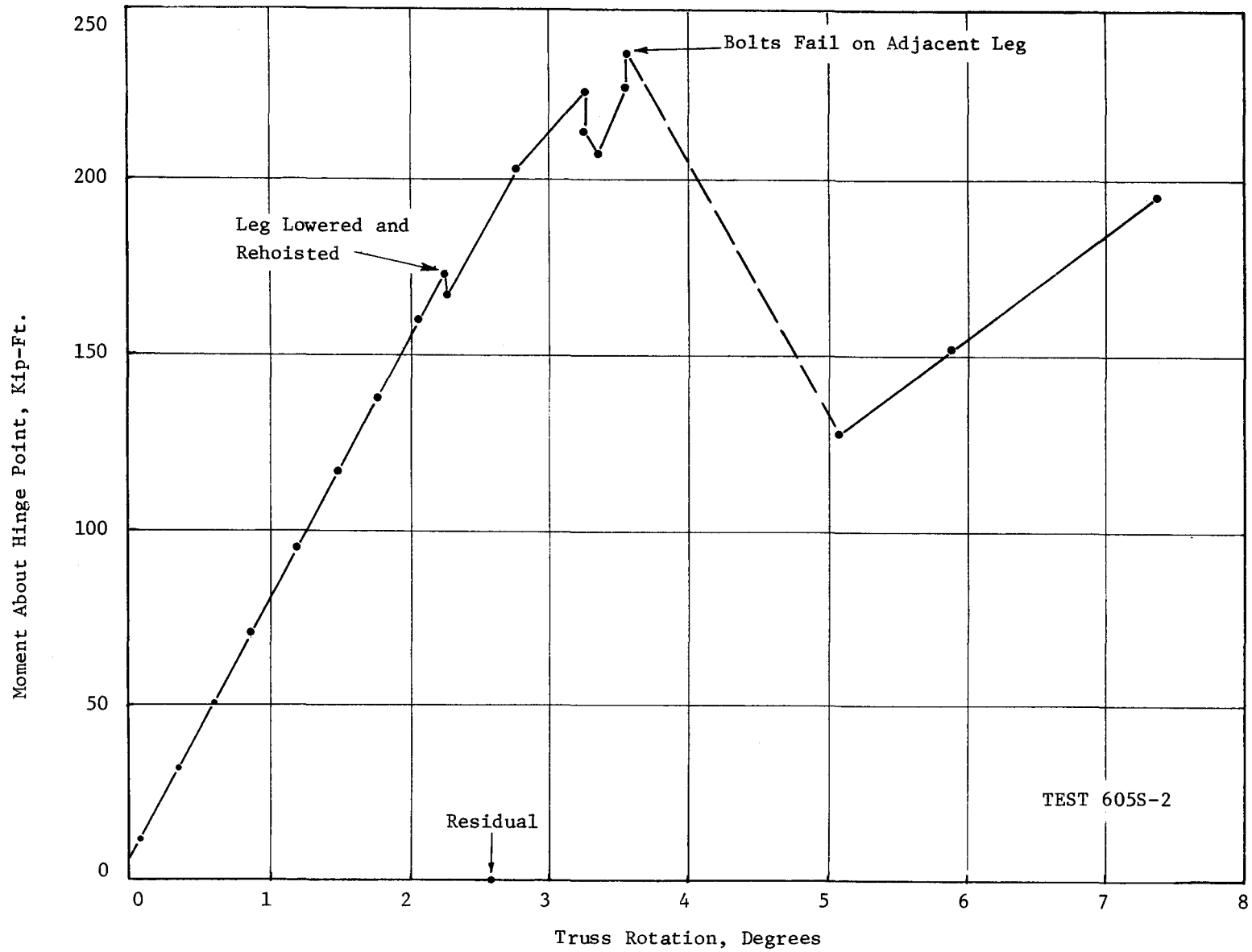
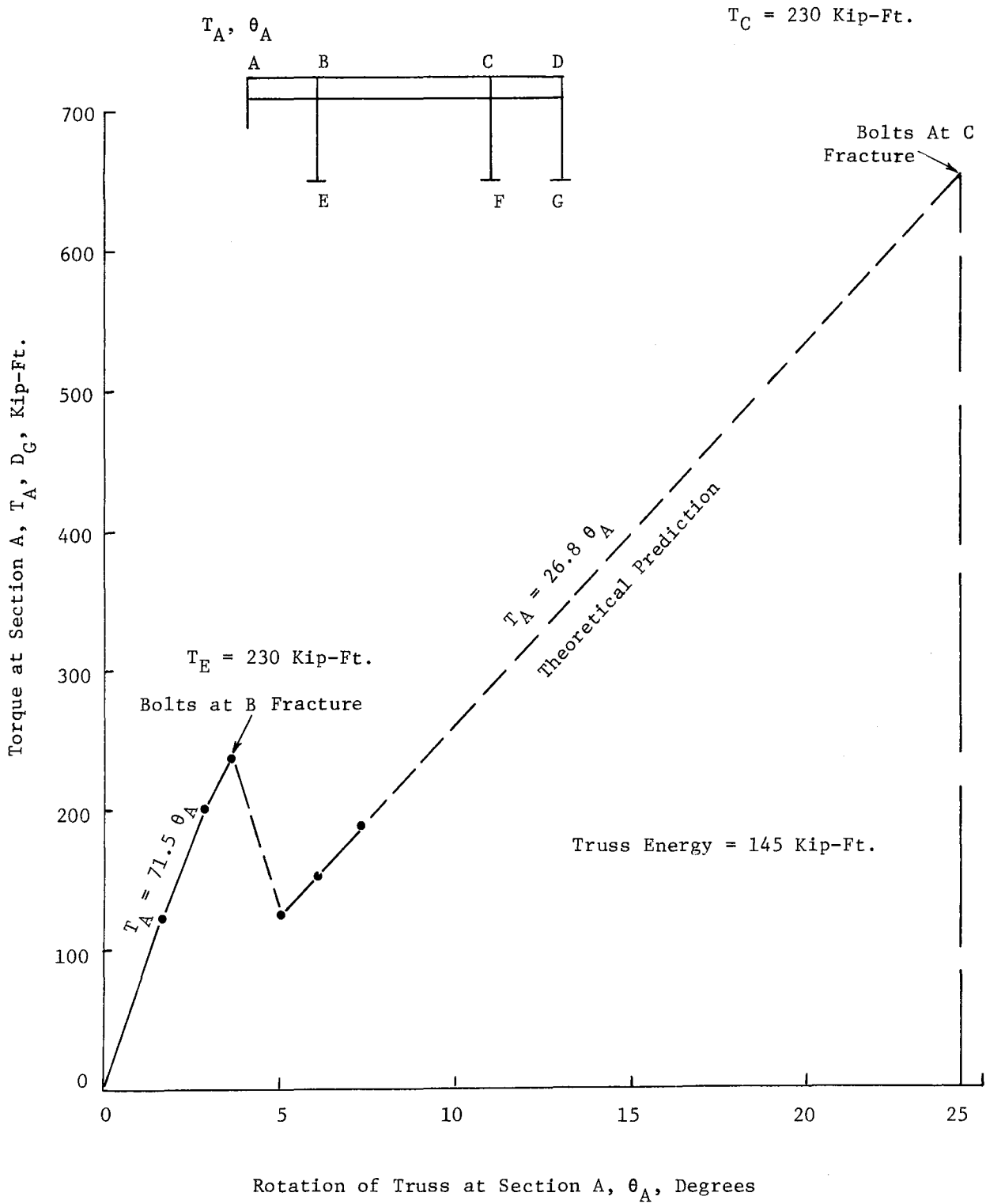


Figure 26, Applied Moment Versus Truss Rotation.



Rotation of Truss at Section A, θ_A , Degrees

Figure 27, Torque-Rotation Relationship.

results of the analysis indicate the following: the torsional stiffness of a 20-foot segment of the OSB truss is 79 kip-ft per degree rotation. The resistance of a single support before failure of the upper bolt connection was previously found by conventional analytical methods to be 750 kip-ft per degree. Based on the results of this test, the torsional stiffness coefficient of Support B after failure of the upper connection bolts was found to be 24 kip-ft per degree. Based on these stiffness coefficients, and the empirically determined moment necessary to produce failure of upper connection bolts at any support (230 kip-ft), a torque versus truss rotation curve was constructed for an applied torque at Support A up the point where the bolts at the upper connection of Support C fail. This curve is shown in Figure 27, and indicates that the OSB may absorb 145 kip-ft of energy before the failure of all upper connection bolts takes place. This calculation assumes that no inelastic action takes place within the Overhead Sign Bridge and is based on the extrapolation of a very limited amount of data. Therefore, the actual magnitude of the energy found is subject to considerable question. The indications are, however, that the truss may be able to absorb at least the 80 kip-ft of energy predicted for the impact of a 5,000 pound vehicle traveling 60 mph. Test 605-S2 indicated that vehicle crash testing may be conducted at higher speeds without severe damage to the OSB.

Figure 28 illustrates the OSB behavior at 190 kip-ft static moment and a rotation of 7.4°.

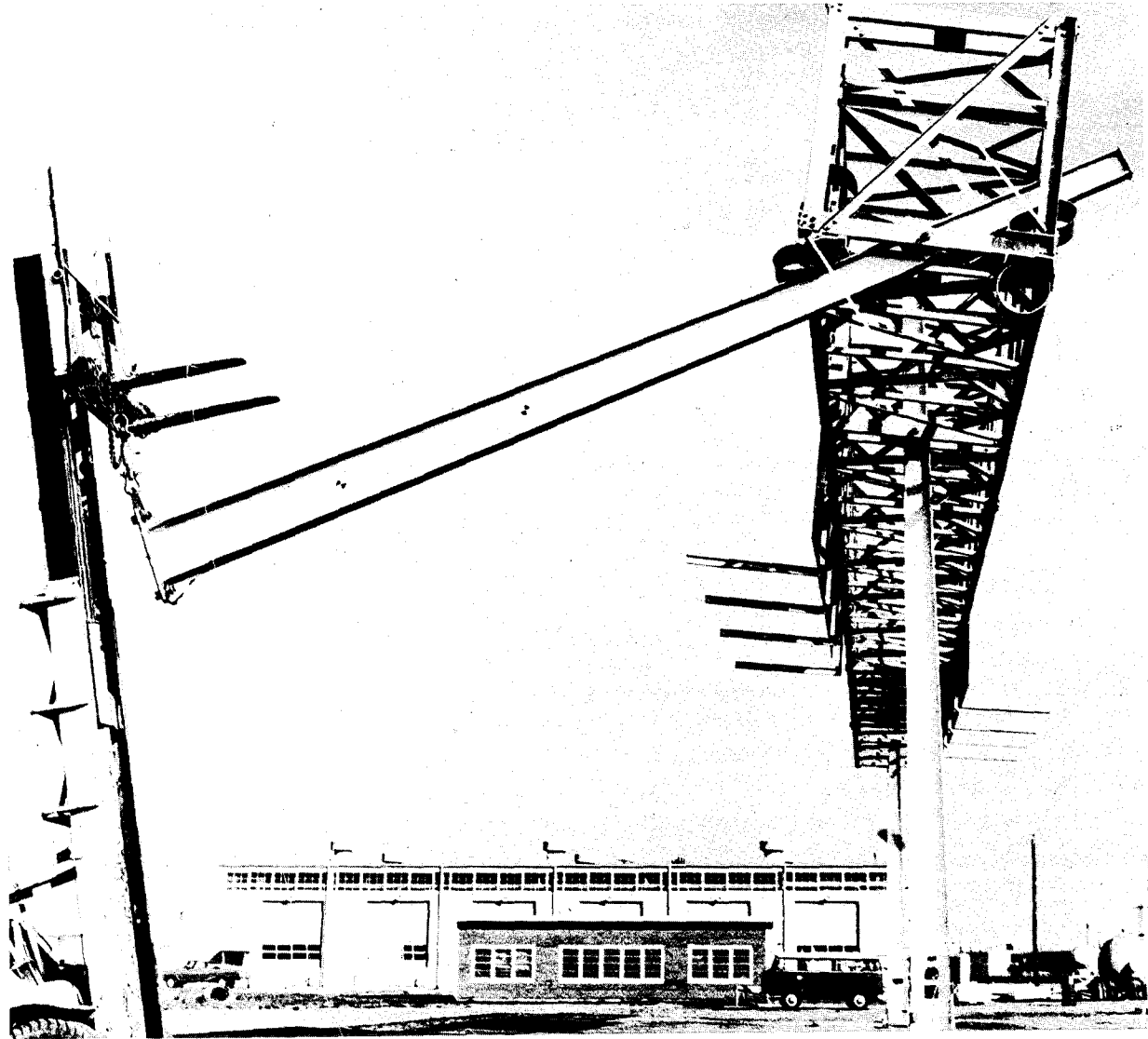


Figure 28, Dead Load Test of Prototype Structure.

TABLE 5

INSTRUMENTATION FOR STATIC LOAD TESTS OF OSB

Test 605-S1

Load Readings	1. Bourdon Tube Hydraulic Gage on loading ram.
	2. SR-4 load reading from strain gage load cell.
Slip Readings	1. 1/1000 inch dial indicator used for first two inches of slip.
	2. Direct reading scale attached to base plate for values of slip between 2 and 14 inches.
Truss Deflection	Transits focused on upper and lower truss elements to record deflection and rotation.

Test 605-S2

Load Readings	SR-4 load reading from strain gage load cell.
Support Movement	Indirect measurement, using steel tape, of change in distance from bottom of support Leg A to anchor plate on foundation.
Truss Movement	Transits focused on upper and lower truss elements to record deflection and rotation.
Energy Absorber Deflection	Transits focused on scales adjacent to tubular energy absorbers to record deflections.

LOWER CONNECTION LABORATORY TESTS

Tests 605-LC

The purpose of this series of static load tests was to determine the influence of three parameters on the force variation during slippage and the energy necessary to activate or slip the lower connection of the break-away OSB support. The parameters are: (1) bolt torque, (2) axial load, and (3) bolt keeper plate configuration. The test conditions for the series of ten tests are given in Table 6.

An investigation of these parameters was suggested by static load test 605-S1 reported earlier (see page 30, et seq.). The vagaries of estimating friction and fracture forces are well known, and thus lab tests become necessary to provide basic information for mathematical simulation and for design purposes. It is recognized that such tests provide load-slip information under slowly applied loads, whereas vehicle collisions produce rapid load application. However, previous experience has led to the conclusion that static load data can be employed in mathematical simulation with some degree of success (see Technical Memorandum 605-1), and thus these tests further clarify the otherwise unknown load-slip behavior of the break-away base and keeper plate.

Examination of Table 6 reveals that seven tests were conducted without a bolt keeper plate, and three with selected keeper plates. Test results are plotted in the figures indicated in the table. The test apparatus is illustrated in Figure 29, a test in progress is

TABLE 6

LOWER CONNECTION LABORATORY TESTS

TEST NUMBER	AXIAL LOAD (kips)	BOLT TORQUE (ft-lbs)	KEEPER TYPE	TEST RESULTS SHOWN IN FIGURE NUMBER
605LC-1	5.5	0	None	32
2	11.2	0	None	32
3	22.7	0	None	32
4	0	50	None	33
5	0	100	None	33
6	0	200	None	33
7	0	400	None	33
8	0	0	28 gage (slotted)	34
9	0	0	28 gage	34
10	0	0	20 gage	34

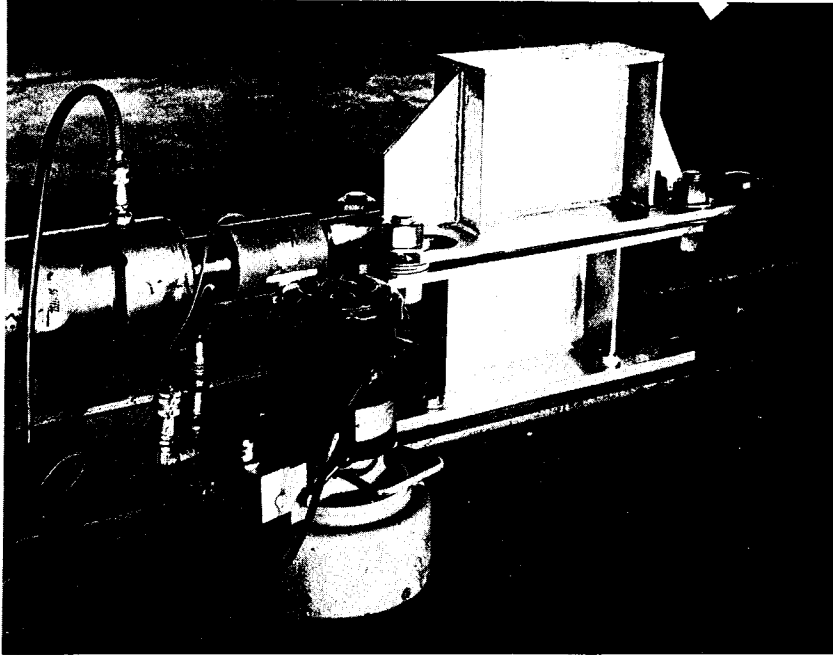
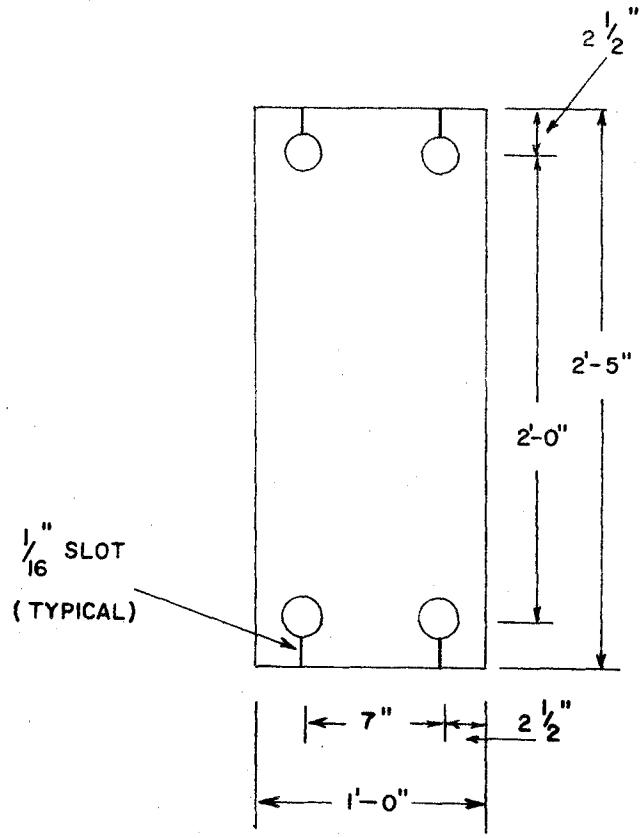


Figure 29, Test Apparatus.

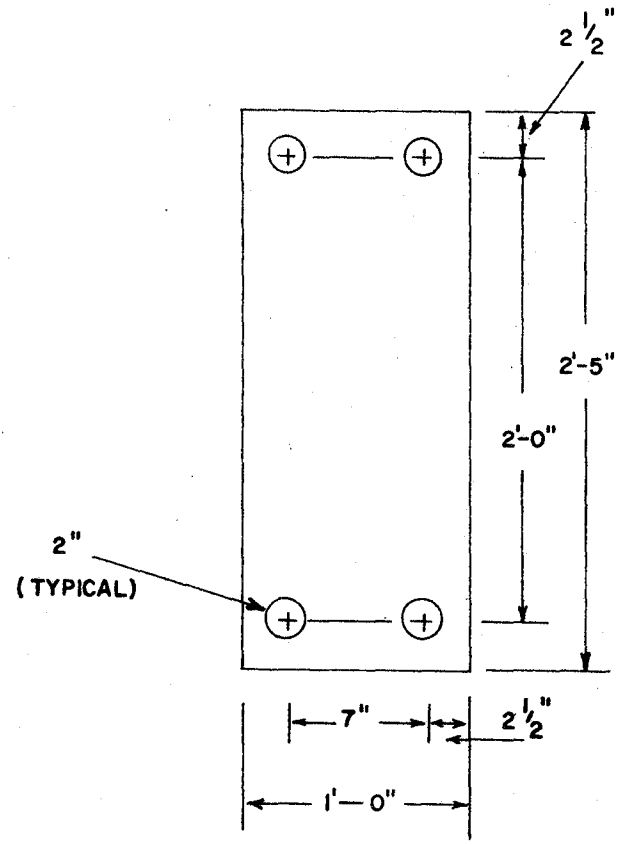
(Note three washers between base plates.)



Figure 30, Test 605 LC-9 in Progress.



TEST 605 LC-8
(28 GAUGE)



TEST 605 LC-9
(28 GAUGE)

TEST 605 LC-10
(20 GAUGE)

FIGURE 31, DETAIL OF KEEPER PLATES.

shown in Figure 30, and details of keeper plates are seen in Figure 31.

The effect of axial load on load-slip characteristics is shown in Figure 32. This series of tests was conducted without a bolt keeper plate, and the bolt torque was zero (bolts were in place and nuts were hand tightened). The ratio of the load required to cause initial slip to initial axial load provides an estimate of the effective coefficient of friction. In this series of tests, the effective coefficient of friction varied between 0.14 and 0.18.

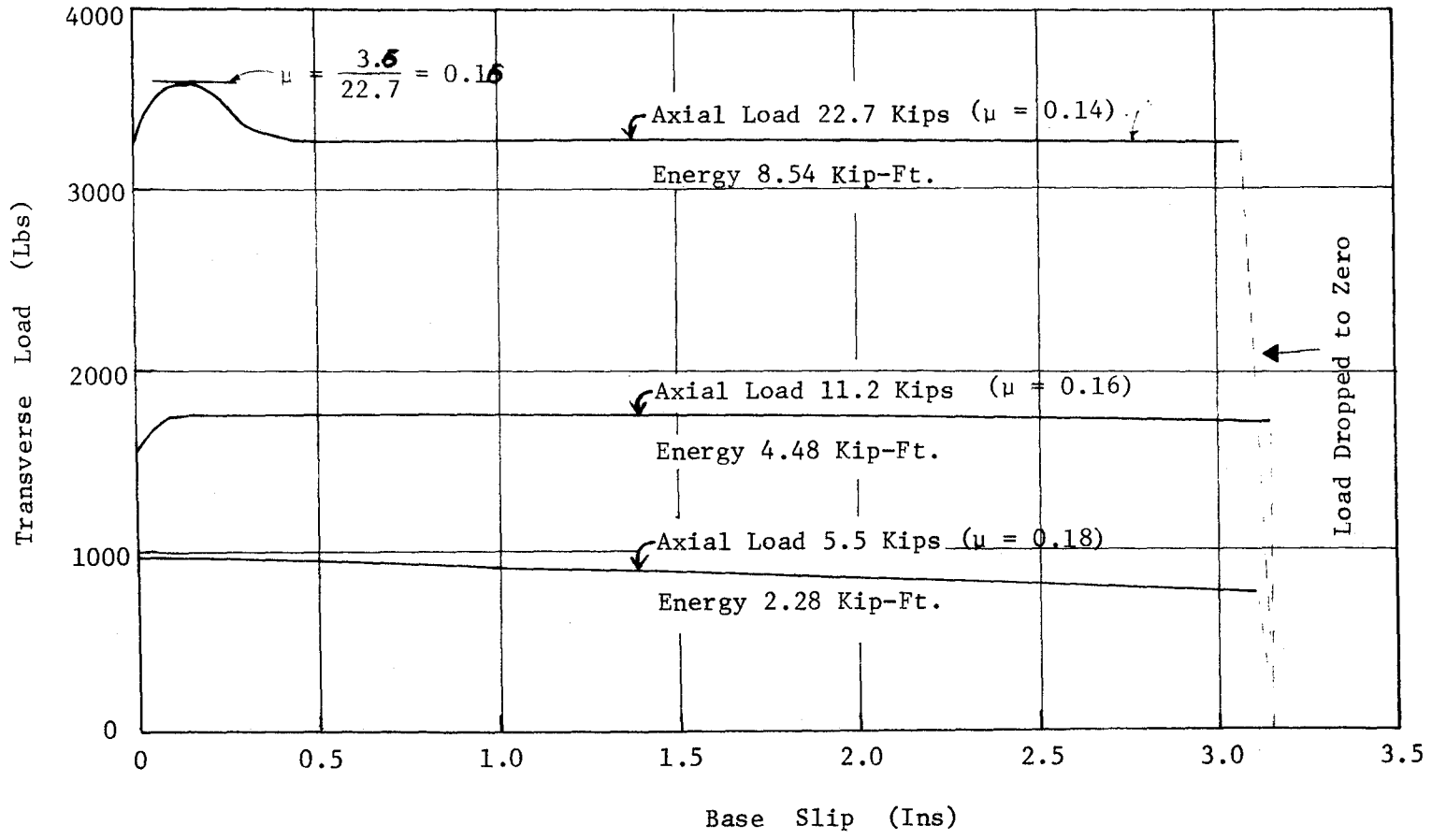


Figure 32, Load-Slip Curves, Tests 605 LC - 1 through 3.

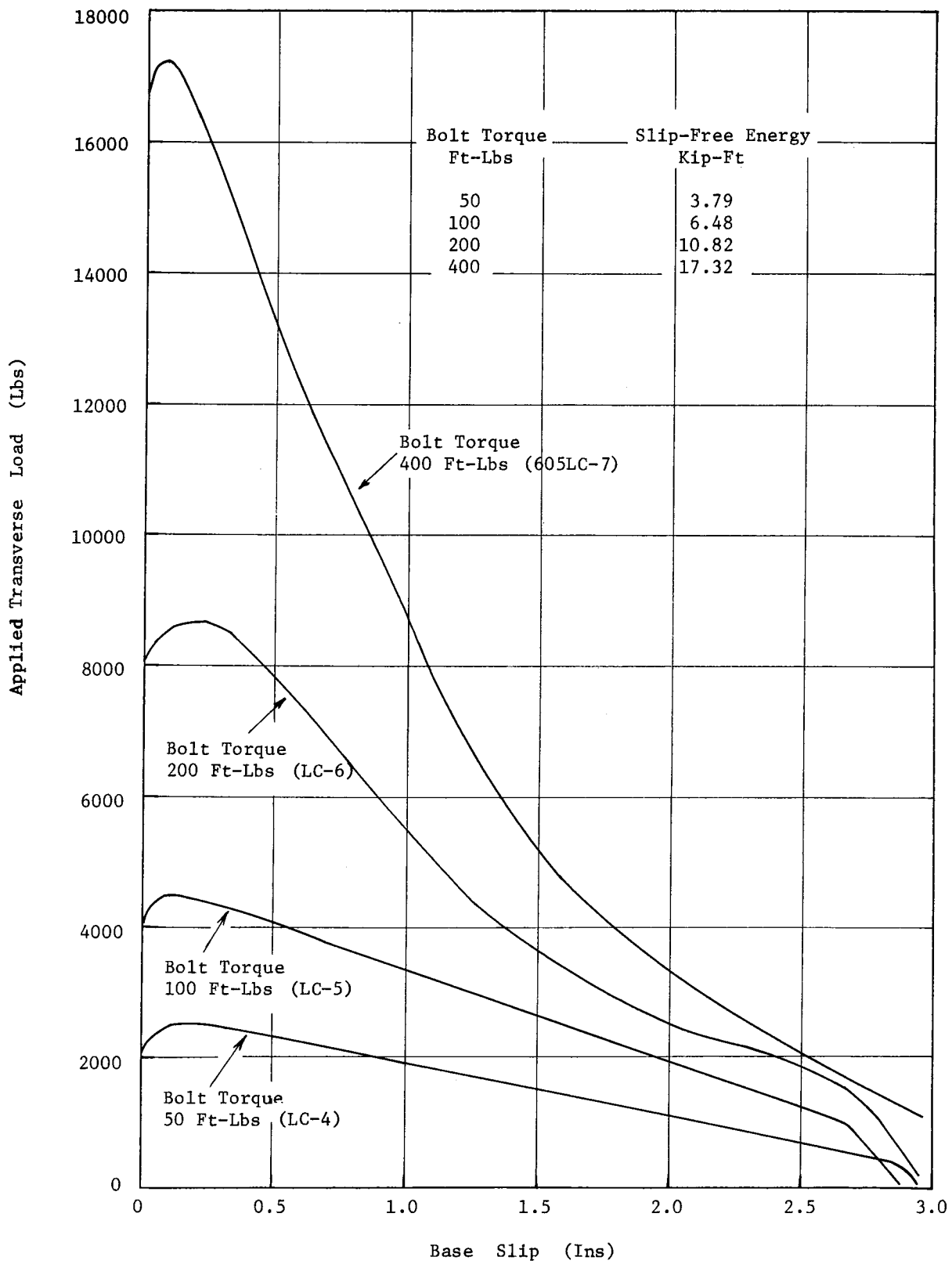


Figure 33, Load-Slip Curves, Tests 605 LC - 4 Through 7.

The effect of bolt torque on the transverse load required to produce slip of the break-away base was investigated, with the results shown in Figure 33. In this series of tests, the axial load was removed, as was the bolt keeper plate. The 1-3/4 inch diameter base bolts were tightened to the specified torque using a torque wrench. The base plates were separated by three washers on each bolt. This tightening procedure corresponded to that employed in tightening the base bolts on the prototype structure.

It is interesting to note that the value at which initial slip occurred is almost directly proportional to the bolt torque in the range tested. The 400 ft-lb torque curve has the largest deviation and is still within 5 percent of being directly proportional. The peak load occurs at a slip of 0.1 inch to 0.2 inches in each test, and the total slip at which the applied transverse load became zero is in each case approximately 3 inches.

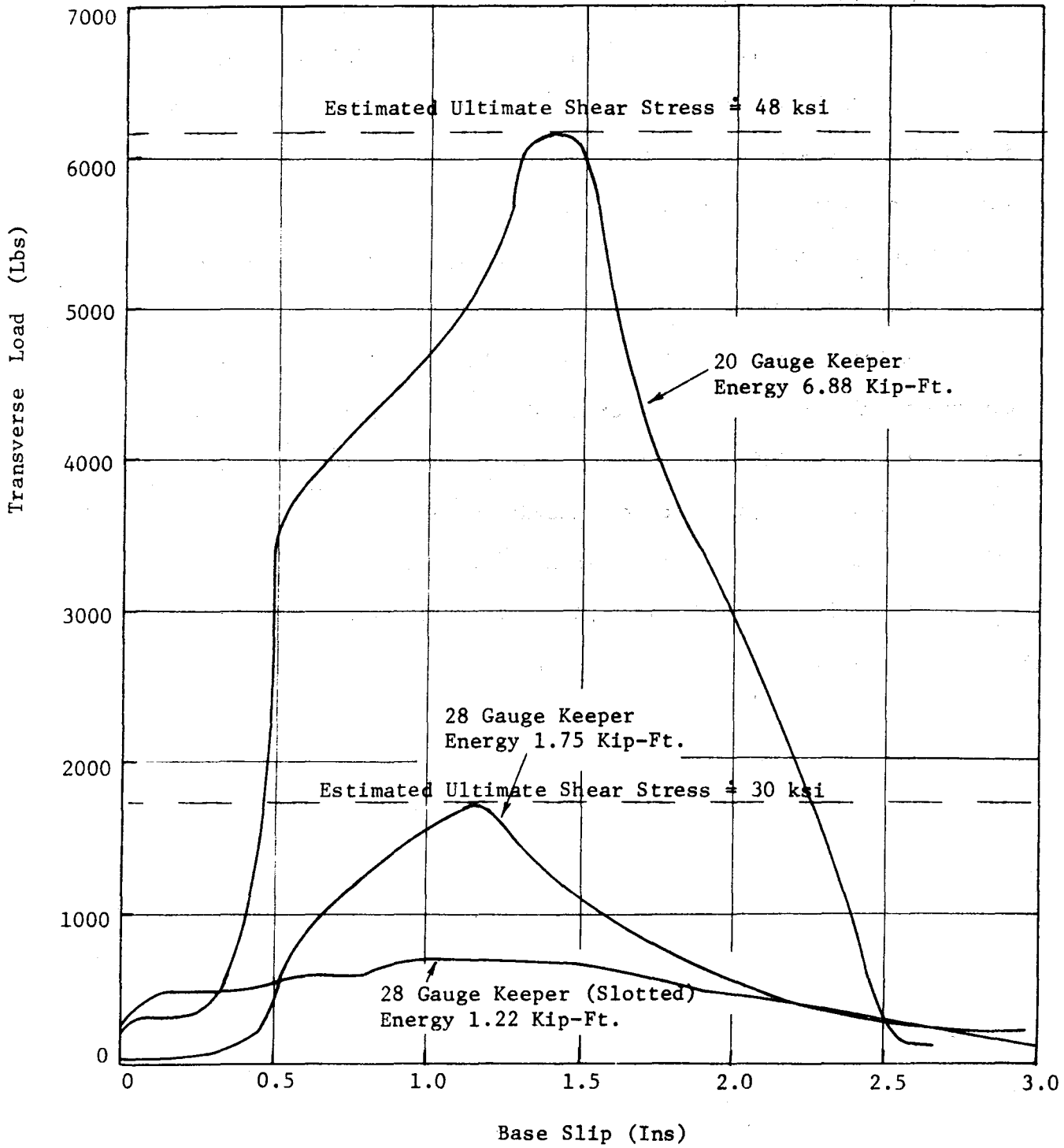


Figure 34, Load-Slip Curves, Tests 605 LC - 8 Through 10.

Finally, the strength of the keeper plate was investigated, with the results shown in Figure 34. In this series of tests, the bolts were hand tightened in place, and no axial load was applied. An estimate of the fracture strength of a keeper plate (assuming direct shear) is shown on the plot of Figure 34. These values, based on the greatly simplified failure mode, appear reasonable. They are based on a nominal 2-inch diameter hole (+ 1/8 inch tolerance). The effective width at tear out, as seen in Figure 39, was actually significantly greater. Also, it is apparent that the mode of failure of the sheet metal was not simple shearing, but was combined with bearing deformation of the metal keeper plate.

The slotted keeper plate was tested to determine the effect of weakening the shear strength of the bolt keeper plate. Such slotting is not believed necessary since the energy required to fracture the 28-gage keeper plate is quite low.

A more convenient form of the data obtained is given by Figures 35, 36, and 37 which show slip-free energy as a function of bolt-torque, axial load, and keeper configuration respectively. The energy necessary to activate a given lower connection under any combination of the three variables should then be found by a simple summation of the individual effects. The energy levels determined by this series of static tests are probably not quantitatively equal to the energy levels that would be found by dynamic tests. It is believed, however, that the relative importance and influence of each parameter are indicated by the static tests.

In addition to the resistance to base slip due to bolt torque, axial load and keeper plate, additional resistance to slip is due to the

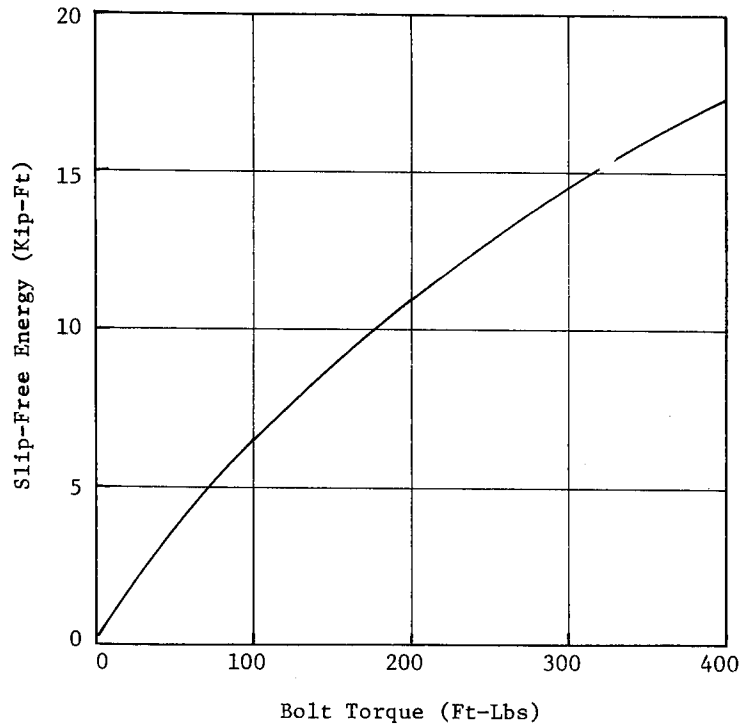


Figure 35, Effect of Bolt Torque on Slip-Free Energy.

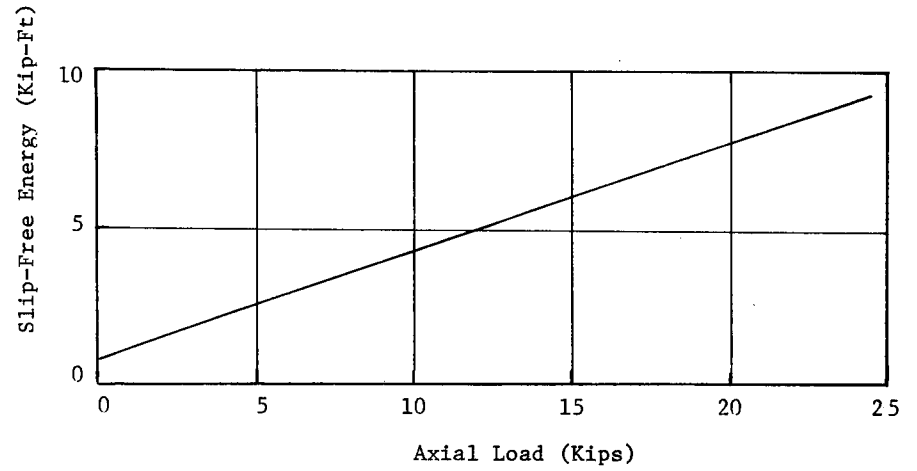


Figure 36, Effect of Axial Load on Slip-Free Energy.

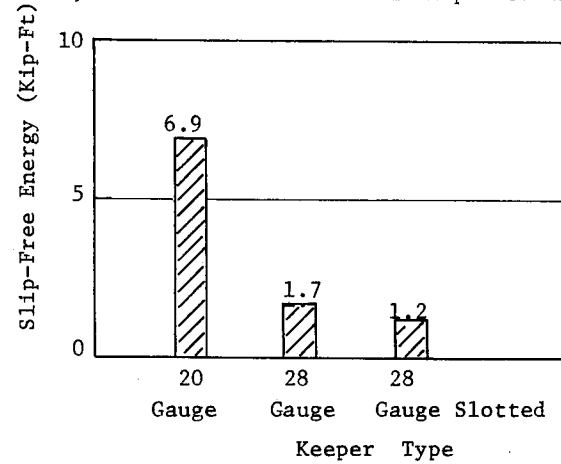
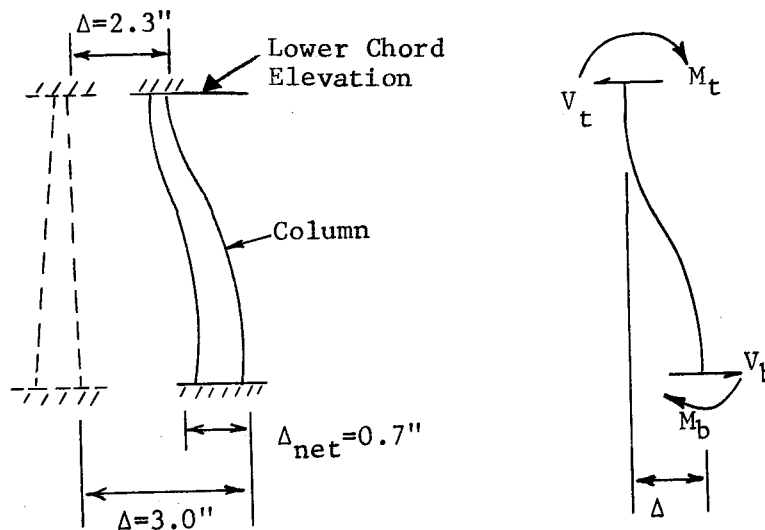


Figure 37, Effect of Keeper Type on Slip-Free Energy.

attachment of a support to the truss. This portion of the resistance approaches zero after the upper connection shears free.

It should be recalled that the support column is connected to the lower chord by a 1-7/16 inch diameter stainless steel pin, which can transmit a horizontal shear force to the truss through the pinned connection, and that a bending moment in the column also exists at this location. Data from Test 605-S1 indicated that the truss, at the column under load, translated in the direction of load without significant rotation up to the point when the base slipped free. At the point when the base slip was 3 inches, the truss had translated 2.3 inches. This suggests that the portion of resistance to base slip due to the rigidity of the truss can be calculated using the following simplified model:



Analysis of this model by slope-deflection technique results in a transverse force at the base, V_b , of 8,000 pounds for a base slip of 3 inches. This force is assumed to vary linearly from zero to zero

base slip to 8,000 pounds at 3 inches of base slip. It can be added to the effects of bolt torque, axial load and keeper from the LC test series.

A comparison of force variation as a function of lower connection slip between static load test 605-S1 and the force versus slip variation determined by the "summation-of-effects" from the LC test series is given in Figure 38. The peak transverse force predicted by the "sum-of-effects" method is approximately 20 percent lower than the maximum force observed in the S1 test. The two methods compare very well in predicting the amount of energy necessary to slip the lower end of the support free. The energy determined from the load-slip curves from Test 605-S1 was 2.54 kip-ft and the energy given by the "sum-of-effects" method was 2.36 kip-ft. The largest discrepancy between the two curves is in the region between 2.5 and 3 inches of base slip. One reason for this may be the slight difference in the way the upper plate moves with respect to the lower plate in Test S1 and in the LC test series. In the S1 test, the upper plate was moving in an arc of very slight curvature and the load was applied approximately 22 inches above the ground, while in the LC test series, the upper plate moved in a straight path and the load was applied directly to the upper plate. Another possible discrepancy is due to the fact that the axial load for the S1 test was assumed to be 8 kips. This assumption could be considerably in error.

In view of these possible variances between the full-scale static load tests on the OSB and the LC test series, the comparison shown in Figure 38 is remarkable. The information obtained from these static tests indicated that the base resistances employed as input to mathematical simulation were reasonable. Thus, the investigators were

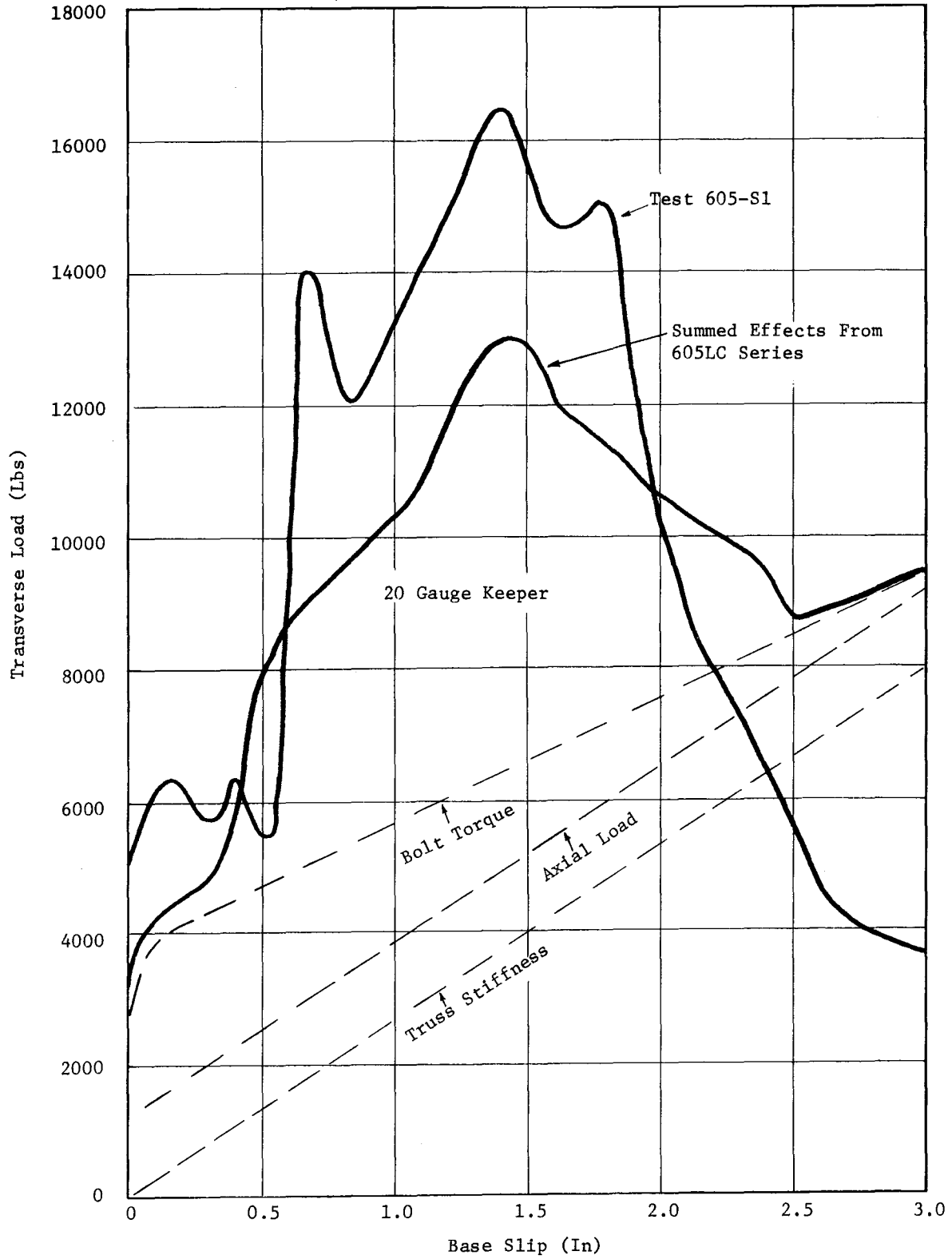


Figure 38, Comparison of Load-Slip Curves for Tests 605-S1 and 605 LC Series.

encouraged to continue the full scale crash testing of the prototype structure. The results predicted by computer simulation are contained in Technical Memorandum 605-2, and have thus far been validated by crash tests conducted and reported in this Technical Memorandum.

* * * * *

The following appendices contain detailed crash test data (Appendix A) and the method used for computing torsional stiffness coefficients (Appendix B).

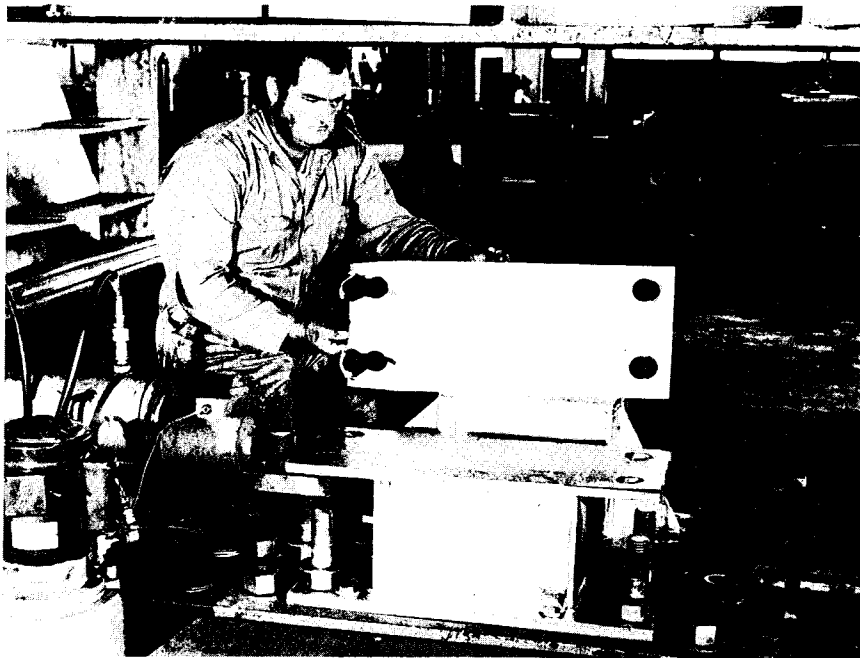


Figure 39, Torn Keeper Plate Used in Test 605 LC-9.

APPENDIX A

TEST DATA

TABLE A1

TEST 605-Y

High Speed Film Data

<u>Time</u> <u>msec.</u>	<u>Displacement</u> <u>ft.</u>	<u>Time</u> <u>msec.</u>	<u>Displacement</u> <u>ft.</u>
		(continued)	
-71.0	-2.2	223.1	5.0
-60.8	-1.9	243.1	5.4
-50.7	-1.6	263.6	5.8
-40.6	-1.2	283.9	6.2
-30.4	-0.9	304.2	6.6
-20.3	-0.6	324.5	7.0
-10.1	-0.3	344.8	7.4
Impact → 0	0	365.0	7.8
10.0	0.3	385.3	8.2
20.3	0.6	405.6	8.6
30.4	0.9	425.9	9.0
40.6	1.1	446.2	9.4
50.7	1.4	466.4	9.8
60.8	1.7	486.7	10.2
71.0	1.9	507.0	10.6
81.1	2.1	527.3	11.0
91.3	2.4	547.6	11.4
101.4	2.6	567.8	11.8
121.7	3.0	588.1	12.2
142.0	3.4	608.4	12.6
162.2	3.8	811.2	16.5
Loss of Contact → 182.5	4.2	1115.4	22.3
202.8	4.6	1521.0	29.8

TABLE A2

TEST 605-A

High Speed Film Data

<u>Time</u> <u>msec.</u>	<u>Displacement</u> <u>ft.</u>	<u>Time</u> <u>msec.</u>	<u>Displacement</u> <u>ft.</u>
		(continued)	
-50.6	-1.9		
-40.5	-1.5	161.9	5.0
-30.4	-1.1	172.0	5.3
-20.2	-0.8	182.2	5.6
-10.1	-0.4	192.3	5.9
Impact → 0	0	202.4	6.2
10.1	0.4	212.5	6.5
20.2	0.7	222.6	6.8
30.4	1.1	232.8	7.1
40.5	1.4	242.9	7.4
50.6	1.7	253.0	7.7
60.7	2.0	263.1	8.0
70.8	2.3	273.2	8.2
81.0	2.6	283.4	8.5
Loss of Contact → 91.1	2.9	293.5	8.8
101.2	3.2	303.6	9.2
111.3	3.5	313.7	9.4
121.4	3.8	323.8	9.7
131.6	4.1	334.0	10.0
141.7	4.4	344.1	10.3
151.8	4.7	354.2	10.6
		364.3	10.9

TABLE A3

TEST 605-B

High Speed Film Data

<u>Time</u> <u>msec.</u>	<u>Displacement</u> <u>ft.</u>	<u>Time</u> <u>msec.</u>	<u>Displacement</u> <u>ft.</u>
		(continued)	
-40.4	-2.6		
-30.3	-2.0	171.7	8.1
-20.2	-1.3	Front Wheels Leave Ground	
-10.1	-0.7		
Impact → 0	0		
10.1	0.7		
20.2	1.3		
30.3	1.8		
40.4	2.3		
50.5	2.7		
60.6	3.2		
70.7	3.6		
80.8	4.1		
90.9	4.5		
101.0	5.0		
111.1	5.4		
121.2	5.8		
131.3	6.3		
141.4	6.8		
151.5	7.2		
161.6	7.7		

TABLE A4
TEST 605-C

High Speed Film Data

<u>Time</u> <u>msec.</u>	<u>Displacement</u> <u>ft.</u>	<u>Time</u> <u>msec.</u>	<u>Displacement</u> <u>ft.</u>
		(continued)	
-50.0	-3.4		
-40.0	-2.7	150.0	8.5
-30.0	-2.1	160.0	9.1
-20.0	-1.4	170.0	9.7
-10.0	-0.7	180.0	10.2
Impact → 0	0	Loss of Contact	
10.0	0.6	190.0	10.7
20.0	1.3	200.0	11.3
30.0	1.9	210.0	11.9
40.0	2.6	220.0	12.4
50.0	3.1	230.0	12.9
60.0	3.6	240.0	13.5
70.0	4.1	250.0	14.1
80.0	4.7	260.0	14.6
90.0	5.2		
100.0	5.7		
110.0	6.3		
120.0	6.9		
130.0	7.4		
140.0	8.0		

TEST 605-Y

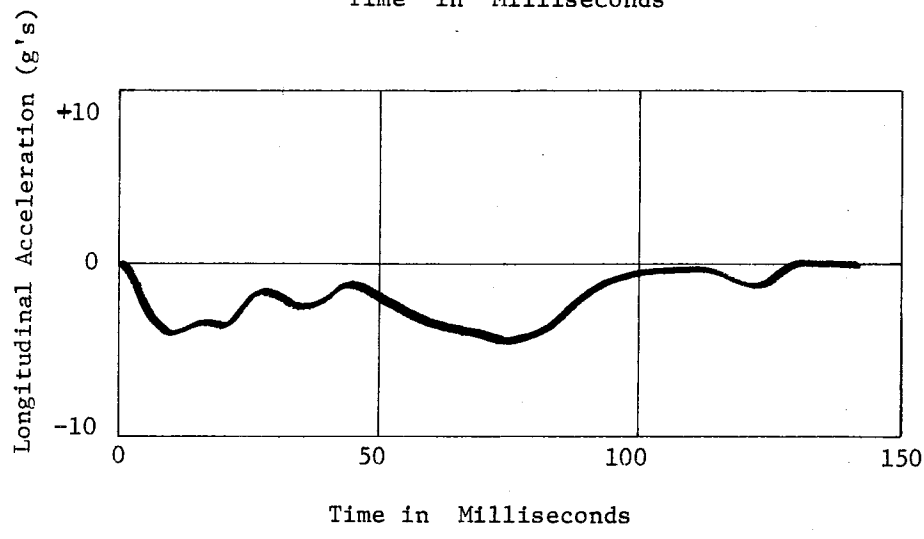
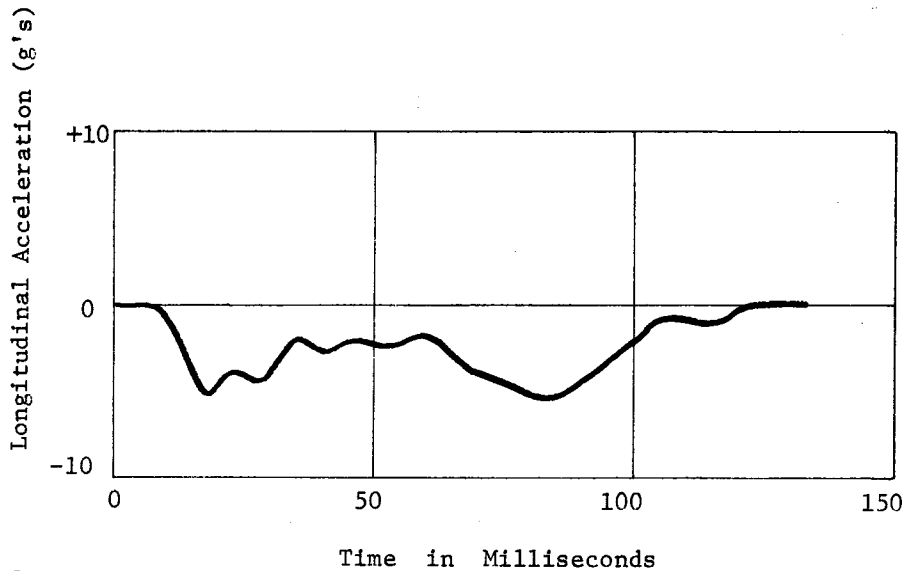


Figure A1, Longitudinal Accelerometer Data

TEST 605-A

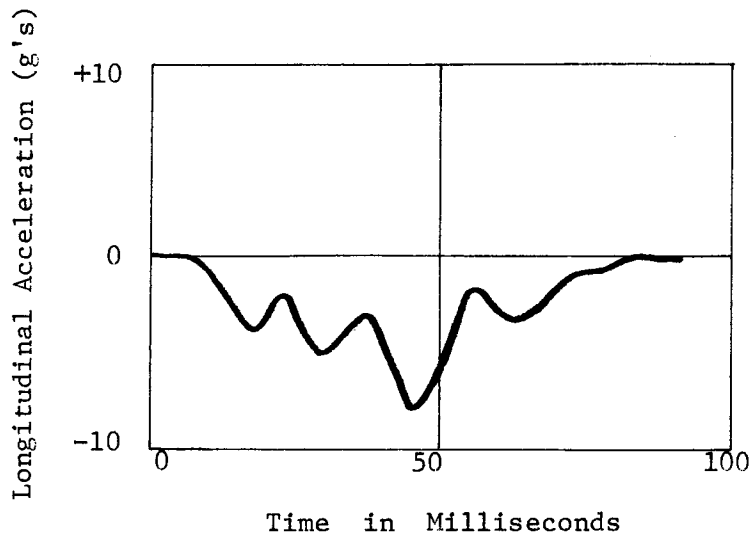
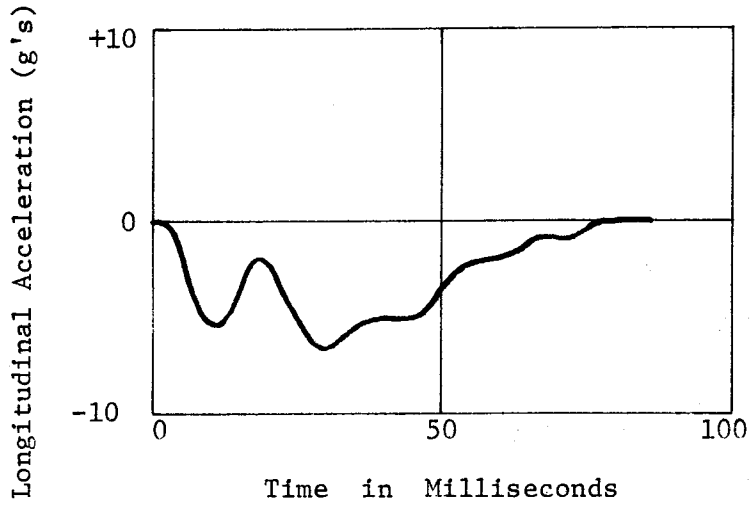


Figure A2, Longitudinal Accelerometer Data

Statham 11081 (left)
80 HZ Filter
Average = 10.1 g's
Peak = 23.4 g's
 $\Delta t = 67.6$ msec

TEST 605-B

Statham 12186 (right)
80 HZ Filter
Average = 9.2 g's
Peak = 21.5 g's
 $\Delta t = 68.1$ msec

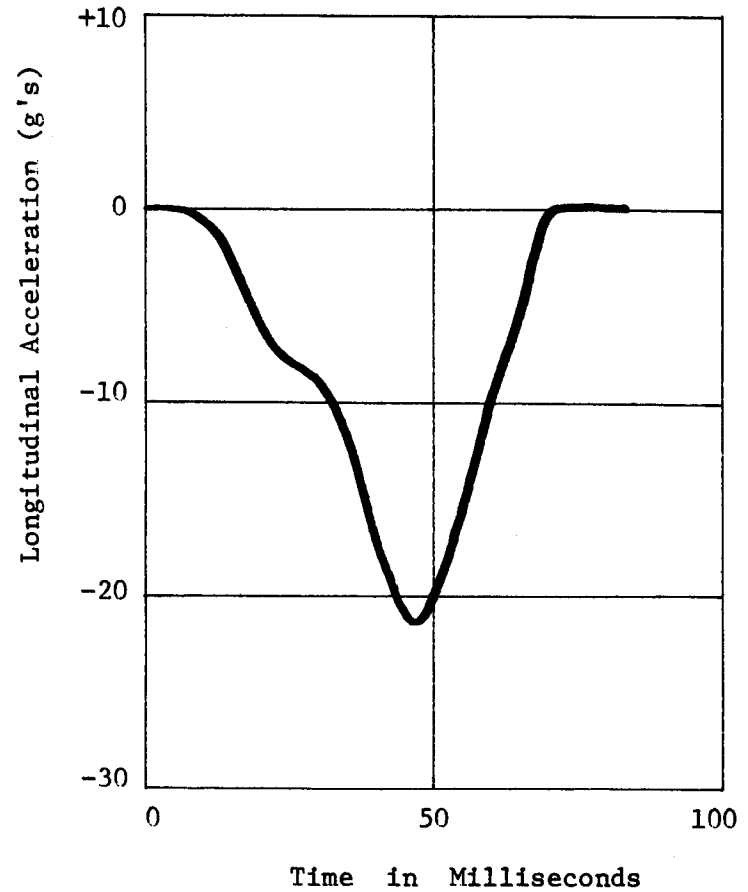


Figure A3, Longitudinal Accelerometer Data

TEST 605-C

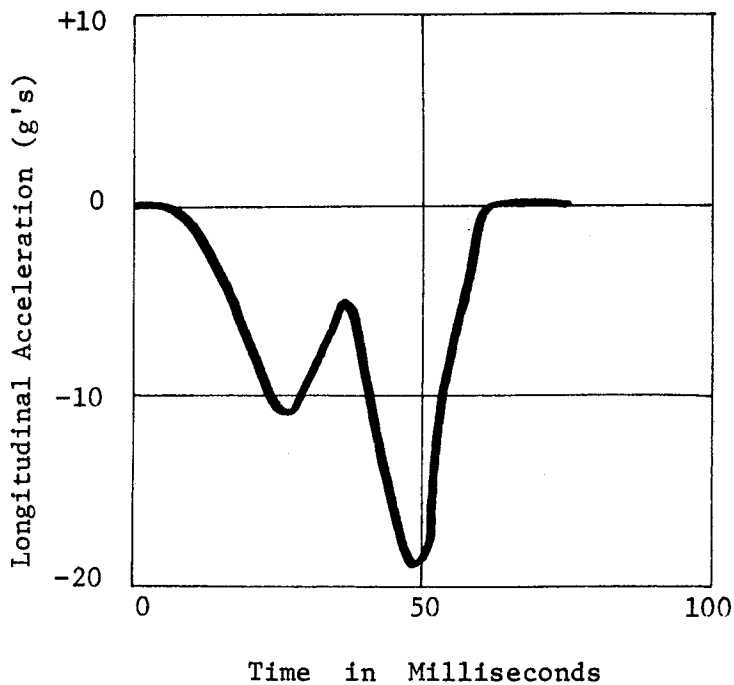
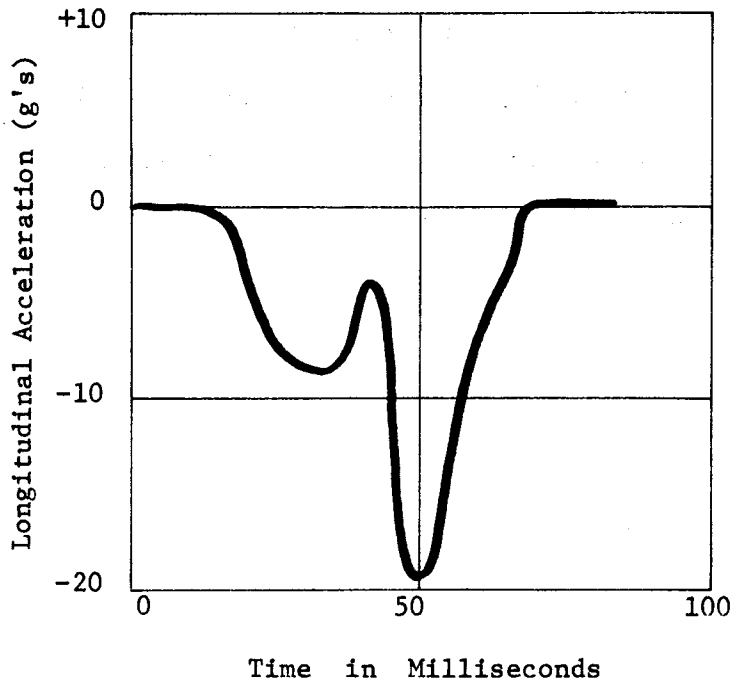


Figure A4, Longitudinal Accelerometer Data

COMMENT

Preliminary observations indicate that there may be a correlation between some events observed in the high-speed films (such as pole-base and top breakaway) and the peaks on the accelerometer traces. A further investigation is being conducted.

APPENDIX B

DETERMINATION OF TORSIONAL STIFFNESS COEFFICIENTS

I. Equilibrium Equations

The overhead sign bridge can be simulated as shown in Figure B1. The assumption is made that the support at point A has been broken free at the base and is applying a torque (T_A) at point A. All torques shown in Figure B1 are in planes perpendicular to the longitudinal axis of the truss.

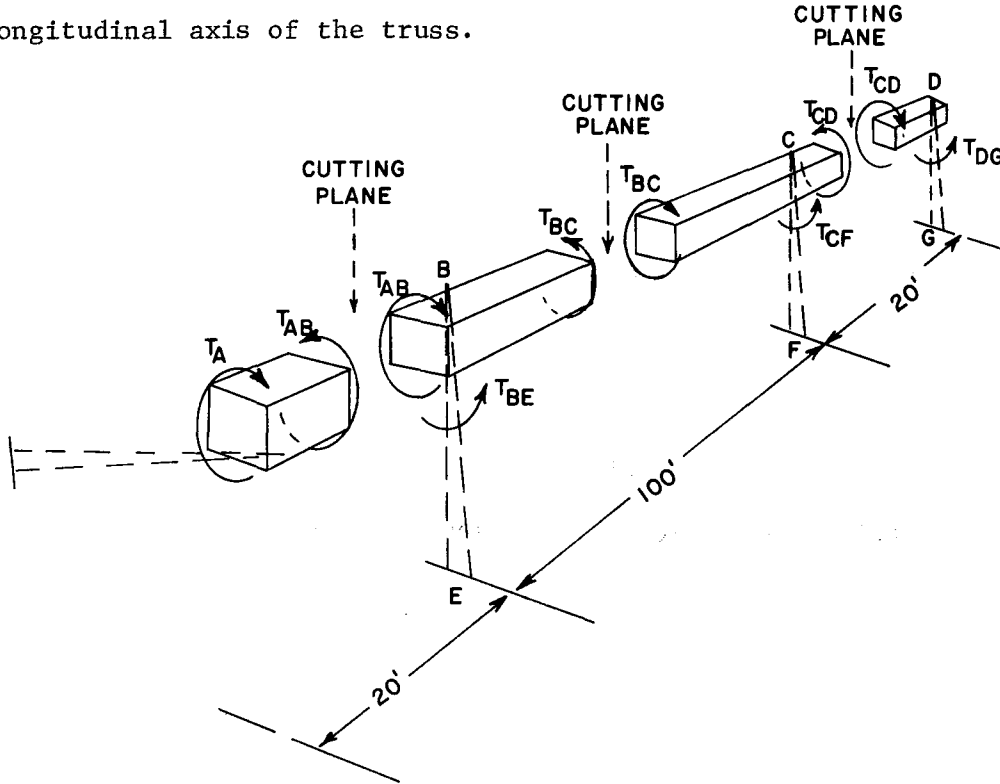


Figure B1, Torsional Loads on OSB Truss.

T_A is the externally applied torque at point A. T_{AB} , T_{BC} and T_{CD} are the torques within the truss between points AB, BC and CD, respectively. T_{BE} , T_{CF} and T_{DG} are the resisting torques applied by the OSB supports at points B, C and D, respectively. By taking a summation of torques about the axis of the truss for the free bodies indicated in Figure B1, the following equations may be written.

$$T_A = T_{AB}, \quad T_{AB} = T_{BC} + T_{BE}$$

$$T_{BC} = T_{CD} + T_{CF}, \quad T_{CD} = T_{DG}$$

$$T_A = T_{BE} + T_{CF} + T_{DG}$$

II. Compatibility Equations

Using a line diagram representation of the OSB in Figure B2, the rotations (θ 's) of various planes in the truss may be defined. A rotation, with a single subscript (e.g. θ_A) defines the total rotation of the truss at point A with respect to its position under no load. A rotation with a double subscript (e.g. θ_{AB}) defines the rotation of the truss at point A with respect to the position of the truss at point B (i.e., relative rotation of A with respect to B).

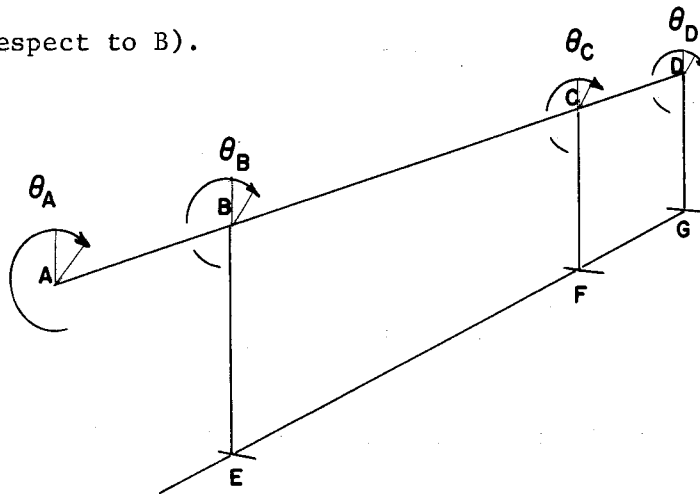


Figure B2, Torsional Displacements of OSB Truss.

Using the displacement diagram shown in Figure B2, the following compatibility equations can be written.

$$\theta_B = \theta_{BE}, \quad \theta_C = \theta_{CF}, \quad \theta_D = \theta_{DG}$$

and

$$\theta_A = \theta_{AB} + \theta_{BC} + \theta_{CD} + \theta_D.$$

The equilibrium and compatibility equations may be related by stiffness coefficients.

i.e.:

$$T_{AB} = K_{AB} \theta_{AB}, \quad T_{BC} = K_{BC} \theta_{BC}$$

$$T_{CD} = K_{CD} \theta_{CD}, \quad T_{BE} = K_{BE} \theta_B$$

$$T_{CF} = K_{CF} \theta_C \quad \text{and} \quad T_{DG} = K_{DG} \theta_D$$

Note: The torsional stiffness of a 20 foot segment of the truss is designated K_2 ,

$$K_2 = K_{AB} = K_{CD} = 5 K_{BC}$$

The resistance of the supports to rotations of the truss is designated K_s ,

and

$$K_s = K_{BE} = K_{CF} = K_{DG}$$

Manipulation of the equilibrium and compatibility equations will yield the following two equations:

$$T_A = T_{DG} (5M^2 + 12M + 3) \quad (1)$$

and

$$\theta_A = \frac{T_{DG}}{K_s} (5M^3 + 17M^2 + 14M + 1) \quad (2)$$

where $M = \frac{K_s}{K_2}$

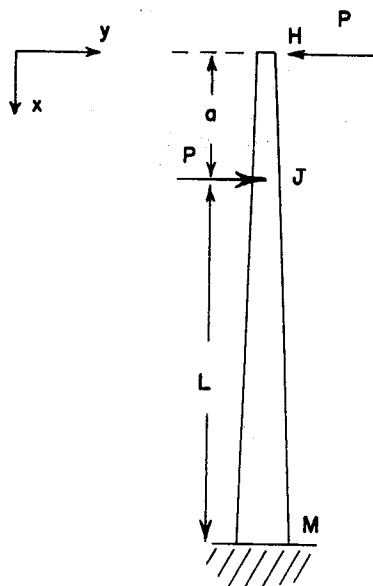
Eliminating T_{DG} from these two equations yields

$$\frac{T_A}{\theta_A} = \frac{K_s (5M^2 + 12M + 3)}{(5M^3 + 17M + 14M + 1)} \quad (3)$$

K_s may be determined using the model shown in Figure B3, using conventional techniques to arrive at the needed deflections.

This was done, and K_s was found to be

$$750 \frac{\text{Kip-Ft}}{\text{Degree}}$$



Moment of Inertia, I_x , Variable

Equations:

$$T = P a$$

$$\Delta_J = \int_a^{a+L} \frac{M_x}{EI_x} dx$$

$$\Delta_H = \int_0^{a+L} \frac{M_x}{EI_x} dx$$

$$\tan \theta = \frac{\Delta_H - \Delta_J}{a}$$

$$K_s = \frac{T}{\theta}$$

Figure B3, Model Used to Calculate K_s .

Now since K_s is known, if values of T_A and θ_A are determined experimentally, the value of M will be determined by equation (3).

Using values of $T_A = 200$ kip-ft when $\theta_A = 2.8^\circ$ (Data from Test 605-S2), the value of M was found to be 9.52

Then

$$M = \frac{K_s}{K_2}$$

and

$$K_2 = \frac{K_s}{M} = \frac{750}{9.52}$$

$$K_2 = 79 \frac{\text{kip-ft}}{\text{degree}}$$

Now, putting the values of K_2 and K_s into equation (3), the T_A θ_A relationship for the first part of Test 605-S2 can be found.

$$T_A = 71.5 \theta_A \quad \left\{ \begin{array}{l} \text{Before failure of} \\ \text{upper connection} \\ \text{bolts at Support B.} \end{array} \right\} \quad (4)$$

Torque in kip-ft

θ in degrees

Now, it is necessary to find the value of the torque, T_{BE} , when the upper connection bolts at Support B failed.

Substituting in the final equilibrium equation we have

$$T_A = T_{DG} + K_s T_{DG} \left(\frac{1}{K_2} + \frac{1}{K_s} \right) + T_{BE}$$

From equation (2)

$$T_{DG} = \frac{\theta_A K_s}{(5M^3 + 17M^2 + 14M + 1)}$$

Empirical values of θ_A and T_A , when the bolts at Support B failed, were 3.6° and 236 kip-ft, respectively. By substituting these values and eliminating T_{DG} , the value of T_{BE} is found to

be 231 kip-ft. Now, to develop the torque-rotation relationship beyond the point of upper bolt failure at Support B, it is necessary to determine the effective torsional restraint offered the truss by Support B after upper connection failure. This stiffness is designated K_{sB} , and is found from the empirical data of Test 605-S2 in much the same way that K_s was originally found. The difference is that K_{sB} must be kept separate from the other K_s values since it now represents some reduced torsional stiffness coefficient.

A modified form of equation (3) with K_{sB} kept separate is

$$\frac{T_A}{\theta_A} = \frac{\left[\frac{K_s}{K_2} + 2 + K_{sB} \left\{ \frac{5}{K_2} \left(\frac{K_s}{K_2} + 2 \right) + \frac{1}{K_2} + \frac{1}{K_s} \right\} \right]}{\left[\frac{1}{K_2} \left(\frac{K_s}{K_2} + 2 \right) + \left(1 + \frac{K_{sB}}{K_2} \right) \left\{ \frac{5}{K_2} \left(\frac{K_s}{K_2} + 2 \right) + \frac{1}{K_2} + \frac{1}{K_s} \right\} \right]} \quad (5)$$

Substitution of the known values of K_s and K_2 and corresponding values of θ_A and T_A (7.3° and 193 kip-ft) from the torque-rotation curve of Test 605-S2 after failure of upper connection at Support B, K_{sB} is found to be $24.1 \frac{\text{kip-ft}}{\text{degree}}$.

Putting this value of K_{sB} back into equation (5), the relationship between T_A and θ_A for the truss after failure of upper connection at point B is

$$T_A = 26.8 \theta_A \quad (6)$$

The next item of interest is to determine how far this relationship will hold before the failure of the upper connection at Support C takes place. This failure should occur when the torque imposed by Support C, T_{CF} , reaches 231 kip-ft (the same value that produced failure at Support B). It is necessary then to calculate T_A when $T_{CF} = 231$ kip-ft. From new forms of equations (1) and (2) (keeping T_{CF} and K_{SB} separate), the following equations may be derived:

$$T_A = T_{DG} + T_{CF} + T_{DG} K_{SB} \left\{ \frac{5}{K_2} \left(\frac{K_S}{K_2} + 2 \right) + \frac{1}{K_2} + \frac{1}{K_S} \right\} \quad (7)$$

$$\theta_A = \frac{T_A}{26.8} = \frac{T_{DG}}{K_2} \left(\frac{K_S}{K_2} + 2 \right) + \left(1 + \frac{K_{SB}}{K_2} \right) T_{DG} \left\{ \frac{5}{K_2} \left(\frac{K_S}{K_2} + 2 \right) + \frac{1}{K_2} + \frac{1}{K_S} \right\} \quad (8)$$

Eliminating T_{DG} , substituting $T_{CF} = 231$ kip-ft, and all the known coefficient values allows T_A to be calculated:

$$T_A = 654 \text{ kip-ft}$$

From equation (6)

$$\theta_A = \frac{654}{26.8} = 24.4^\circ$$

With these corresponding values of T_A and θ_A , the torque-rotation relationship of the OSB can be plotted up to failure of the upper connection bolts at Support C. This is done in Figure B4. The area under this curve, with the abscissa expressed in radians is the amount of energy the truss can absorb. This was found to be

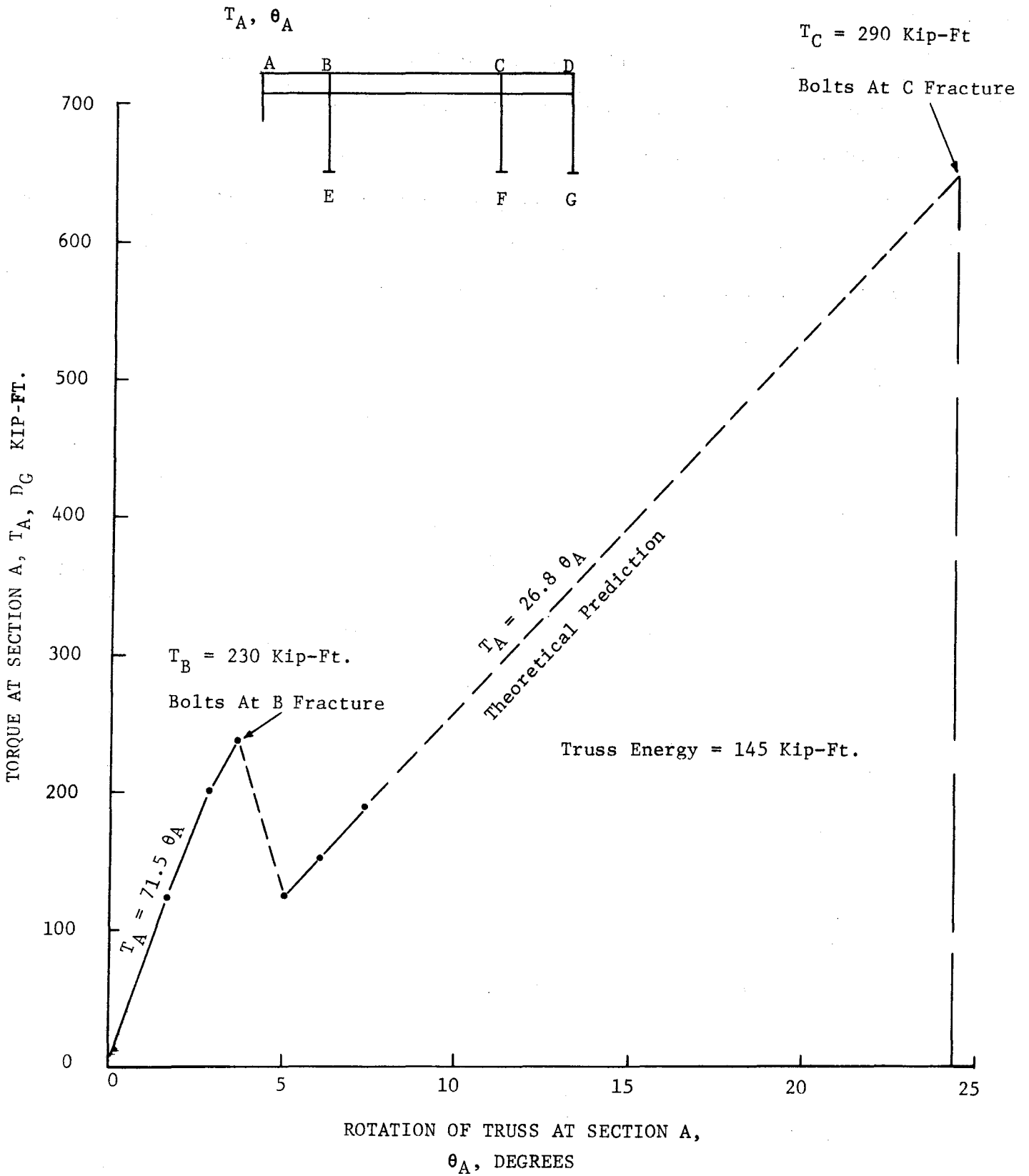


Figure B4, Torque-Rotation Relationship.

145 kip-ft (up to connection failure at Support C). This analysis precludes any inelastic action within the truss and is tenuously based on the extrapolation of a very limited amount of data beyond the point of Support B upper connection failure. It is felt to be indicative that the OSB will probably be able to accommodate the 80 kip-ft of energy imparted by Support A during a 5000-pound -- 60 mph collision.